CONDITIONS AND CHARACTERISTICS OF THE DEVELOPMENT OF THE CHEMICAL COMPOSITION OF HIGHLY MINERALISED MINE WATER OVER A THREE-YEAR PERIOD FOLLOWING THE FLOODING OF THE MANÓ – GABRIELA SIDERITE MINE IN NIŽNÁ SLANÁ

CONDITIONS AND CHARACTERISTICS OF THE DEVELOPMENT OF THE CHEMICAL COMPOSITION OF HIGHLY MINERALISED MINE WATER FROM THE MANÓ – GABRIELA SIDERITE MINE IN NIŽNÁ SLANÁ DURING THREE YEARS AFTER FLOODING

Peter Bajtoš

ABSTRACT

The chemical composition and discharge rate of highly mineralised mine water flowing from the Manó – Gabriela siderite mine (Slovak Ore Mountains, eastern Slovakia) were monitored from the complete flooding of the mine in February 2022 until the end of 2024. The discharged mine water, characterised by a low pH (5.0–5.4), contains extremely high concentrations of sulphates (27–35 $g \cdot L^{-1}$), Mg (4.5–6.1 $g \cdot L^{-1}$), Fe (2.0–4.5 $g \cdot L^{-1}$), Mn (0.2–0.6 $g \cdot L^{-1}$), As (12–19 $mg \cdot L^{-1}$),

Ni (5–20 $mg \cdot L^{-1}$), as well as elevated levels of Co, Al, and Zn, and has caused severe deterioration of water quality in the Slaná River. Statistical analysis revealed a significant downward trend corresponding to the first-flush phenomenon for Fe and Mn over the entire monitoring period. An analysis of the hydrogeological, geochemical, and mining-technical conditions of the mine, supported by geochemical modelling of saturation indices and speciation calculations in PHREEQC, indicates that the anomalously high concentrations of sulphates, Mg, Fe, As, and Ni in the mine water may be linked to the self-heating and spontaneous combustion of pyrite occurring in waste piles of black phyllites in some of the mine workings.

KEY WORDS

Arsenic contamination, pyrite oxidation, spontaneous combustion, mine flooding, black shales

KEY WORDS

Arsenic contamination, pyrite oxidation, spontaneous combustion, mine flooding, black shales

INTRODUCTION

In the 1990s, as a result of the state's phase-out programme in the ore mining sector, mining operations ceased at dozens of ore mines across Slovakia, the majority of which are located in the Spiš-Gemer Ore Mountains (Bajtoš, 2016). System-

systematic monitoring of the chemical composition of mine water, which began to flow out after the mines were flooded, was carried out only on those with the most significant ecological impact. Of these, the most significant ecological impact was caused by the discharge of acidic mine water from the Smolník stratiform pyrite deposit (Lintnerová et al., 2008; Kupka et al., 2012; Bajtoš et al., 2013; Balintová et al., 2023), with a pH of 3–4, total mineralisation (M) 4 $g \cdot l^{-1}$– 16 $g \cdot l^{-1}$, Fe concentration 0.4 $g \cdot l^{-1}$– 1.5 $g \cdot l^{-1}$, Mn 20 $mg \cdot l^{-1}$– 150 $mg \cdot l^{-1}$, sulphates 3 $g \cdot l^{-1}$ – 12 $g \cdot l^{-1}$. The influence of the discharge of acidic

mine water (pH around 3.0, M 1 $g \cdot l^{-1}$, Fe up to 42 $mg \cdot l^{-1}$, Mn = 23 $mg \cdot l^{-1}$ – 42 $mg \cdot l^{-1}$, SO^{2-}_4 = 557 $g \cdot l^{-1}$ – 767 $mg \cdot l)^{-1}$ following the flooding of the Mária copper mine in Rožňava in early 2005 (Tometz, Kyseľová, 2009), on the quality of the River Slaná, though only until the mine's drainage was restored in 2014. Mine water discharges from mines opening up siderite veins for extraction, such as

Ing. Peter Bajtoš, PhD.
State Geological Institute of Dionýz Štúr, Regional Centre Spišská Nová Ves, Markušovská cesta 1, 052 40 Spišská Nová Ves, pet.bajtos@geology.sk

in Slovinky (Bajtoš, 2012; 2024) and Gelnica, Rudňany (Bajtoš, 2022), Novoveska Huta and others, had a slightly alkaline reaction, total mineralisation up to 2 $g \cdot l^{-1}$and a low concentration of Fe. They are environmentally significant – albeit locally in terms of impact – due to their concentrations of As, Sb and Mn.

Since 2011, following the closure of the mining company, spontaneous flooding of the Manó–Gabriela iron mine in Nižná Slaná has been taking place. The rising mine water reached the drainage level in February 2022, and initially low-mineralised and slightly alkaline mine water began to flow into the River Slaná through the Gabriela shaft via the Marta drainage adit. However, after two weeks, its chemical composition changed to acidic water with a pH of 5.0–5.2, M 36 $g \cdot l^{-1}$– 100 $g \cdot l^{-1}$, with concentrations of Fe 3.6 $g \cdot l^{-1}$– 5.1 $g \cdot l^{-1}$, Mn 0.5 $g \cdot l^{-1}$– 0.7 $g \cdot l^{-1}$, sulphates 26 $g \cdot l^{-1}$– 77 $g \cdot l^{-1}$. Concentrations of As, Ni and Co were also extremely high. In addition to the highly mineralised mine water, which significantly adversely affected river water quality, the environmental impact of this event was exacerbated by the precipitation of iron-rich sludge with a high concentration of arsenic in the riverbed, which significantly adversely affected the quality of river sediment (Stríček et al., 2022; 2024) and damaged the river's aquatic ecosystem. Given the urgency of the situation, a state of emergency was declared on the River Slaná in June 2022 in the districts of Rožňava, Revúca and Rimavská Sobota.

As part of the extensive monitoring of the situation that arose, measurements were also taken of the quantity and quality of mine water flowing through the Gabriela shaft from the Manó–Gabriela mine into the Marta drainage adit and subsequently to the surface. Through statistical analysis of the results of this monitoring, this article evaluates its hydrochemical regime for the period from the flooding of the mine in February 2022 to the end of 2024. Geochemical calculations of mine water saturation indices relative to relevant deposit minerals and speciation calculations were performed to explain the main geochemical processes occurring in the Manó – Gabriela, with a focus on explaining the mechanism behind the formation of the unusually high mineralisation of its mine water, with anomalous concentrations of mainly iron, manganese, arsenic, nickel and magnesium. The impact of mine water discharge from the Marta adit on the water quality of the River Slaná and the quality of groundwater in the Quaternary sediments of its riverbed is not – given the complexity of this issue – the subject of this assessment.

MANÓ – GABRIELA MINE IN NIŽNÁ SLANÁ

Iron ore, consisting of metasomatic siderite and ankerite, was mined at the Manó – Gabriela mine. It represents the stratiform type of ore mineralisation in the Gemer region (Grecula et al., 1995). The ore bodies – crystalline limestones with siderite and ankerite deposits – are developed in a phyllite sequence which Bajaník et al. (1984) describe as finely laminated quartz-sericite and graphite-sericite phyllites, forming part of the Bystrý potok Formation of the Gelnica Group (Lower Silurian). Grecula et al. (2009) refer to them as the Holecké layers (part of the Betliar Formation of the Gelnica Group) and describe them as recrystallised black pelitic phyllites with intercalations of lydites, carbonates and volcanic rocks. The Holecké layers outcrop in a NW–SE trend on the southern slope of Rimberk Hill. The Manó–Gabriela mine was excavated within this morphological elevation – a ridge with summit elevations of 618 m a.s.l. and 656 m a.s.l., with mining progressing from the near-surface parts of the deposit, probably as early as the 13th century, towards greater depths (Lukáč, 2002). From 1975, access was provided via the Manó heritage adit and the Manó blind shaft down to the 10th level (197.8 m a.s.l.). The new Gabriela shaft (mouth at 394.8 m a.s.l.) was then extended as far as the 12th level (91.0 m a.s.l.) and has been mined practically down to the 11th level (143 m a.s.l., Mihók, 1997). The River Slaná borders Rimberk Hill to the east at an elevation of 360 m a.s.l. – 355 m a.s.l. Its left-bank tributary – the Kobeliarovský Stream – borders this elevation to the south and west (Fig. 1). The slopes of Rimberk Hill have a gradient of around 25%.

The deposit sequence consists of layers of metasomatic siderite and ankerite, limestone with bituminous admixtures, sericite, quartz and minor phyllite intercalations with lydite. The dip of the strata, and thus of the ore bodies, is 15°–45° to the south in the western part of the deposit, and to the south-south-west and further to the west in the eastern part. In a large part of the deposit, several carbonate bodies are superimposed on one another. The thickest body is the siderite body in the central part of the deposit, with a strike length of approx. 800 m and a dip length of 350 m. Siderite also occurs in other separate bodies with a thickness of 30 to 70 m (Mihók, 1994). In the immediate overburden of the carbonate bodies, black phyllites with layers of bituminous metallidites are found over a large part of the deposit. However, they also occur between the carbonate layers. In the overburden of the deposit sequence, a so-called 'overburden' layer of carbonates with a maximum thickness of 20 m is developed over a smaller area. These are accompanied by black phyllites with lydites, and in places by layers of massive arsenopyrite up to 4 m thick (Mihók, 1994). Turan and Turanová (1993) identified significant differences in the chemical composition of siderite and ankerite from sedimentary deposits ('basic type'), from veins and from black phyllites (referred to here as shales) (Table 1). According to Mihók (1997), the following hypogenic minerals were identified at the deposit: siderite I – IV, ankerite I – IV, quartz I – V, sericite I – III, pyrite I – V, arsenopyrite, gersdorffite I – II, chalcopyrite I – II, ullmanite I – II, dolomite I – II , pyrotite, pentlandite, siegenite (?), milerite, violarite, marcasite, magnetite, sphalerite, tetrahedrite, bournonite, jamesonite, boulangerite, calcite, rutile, zircon, graphite, tourmaline, haematite, kaolinite. The following hypergenic minerals are

described in the deposit (Grecula et al., 1995): goethite Fe^{3+} O(OH), malachite Cu_2 CO_3 $(OH)_2$, azurite Cu_3 $(CO_3)_2$ $(OH)_2$, melanterite Fe^{2+} (SO_4). $7H_2$ O, evansite Al_3 $(PO_4)(OH)_6$ *$6H_2$ O, barite $Ba(SO_4)$, skorodite Fe^{3+} (AsO_4)*$2H_2$ O.

The average concentration of Fe in the mined ore was 33.5%, Mn 2.18%, $_{SiO_2}$ 8.5%, S 0.5%–1.5%.

The main undesirable impurities in the deposit were arsenic, sulphur, lead and zinc, which occur in the form of oxides, sulphides, sulphates and sulphosalts. The average concentration of As in the mined ore, where it is mainly bound in arsenopyrite, ranged from 0.001% to 0.2% (Mihók, 1997a).

The mineral composition of the black phyllites (clayey-siliceous sediments) of the Nižná Slaná deposit is dominated by sericite/illite (50%–75%), quartz and carbonates; the average concentration of organic carbon is 1.26% (Table 2). Illite is occasionally replaced by Mg-chlorite; pyrite and tourmaline are commonly present. From the correlation relationships of trace elements with $C_{org}$and with Th as a typical representative of the detrital fraction, the following groups of elements can be defined (Turanová et al., 1995a):

1) a group of trace elements bound exclusively to the detrital fraction of the investigated black shales: B, Ba, Ti; 2) elements bound to the clay fraction: Sr and Cr; 3) a group of ore elements bound in sulphide minerals with stronger relationships between Co-Ni and Pb-Cu; 4) biogenic V with a very high correlation coefficient to C_{org} (r = 0.90), to which U can also be assigned; free-standing Mn bound predominantly in carbonates. Arsenic occurs in black shales in sulphide form and is likely also bound to organic carbon (Table 3). The presence of arsenopyrite and gersdorfite was also confirmed here by electron microanalysis (Turanová et al., 1992).

The primary hydrothermal alteration of the Manó deposit was weak, as the limestone intercalations and lenses near the surface are almost entirely transformed into siderite and ankerite and therefore did not undergo karstification. The immediate overburden and underburden of the limestone bodies and their metasomatically altered parts consist of phyllites, with lydite intercalations in places. From a hydrogeological perspective, this is a hydrogeological massif with fissure permeability, the degree of which decreases exponentially with depth – from class *V* (fairly weak; according to Jetel's classification, 1982, filtration coefficient $k = 1 \cdot 10^{-6}$ $m \cdot s^{-1}$ – $1 \cdot 10^{-5} m \cdot s^{-1}$) at a depth of 20 m to class *VII* (very weak, $k = 1 \cdot 10^{-8} m \cdot s^{-1}$ – $1 \cdot 10^{-7} m \cdot s^{-1}$) at a depth of 60 m, and negligible below that (Class *VIII* with $k < 1 \cdot 10^{-8} m \cdot s^{-1}$), (Bajtoš in Grecula et al., 2011). Operational records obtained during mining indicate that the main inflows of mine water during mining at the collapse site originated from fault fractures, from old workings above the 6th horizon, and from workings near the Kobeliarov transverse fault, which runs approximately through the centre of the mining field (Homola, Klír, 1975). According to Ščuka (in Lörincz et al., 1989), inflows into the Manó deposit were small and did not exceed 4 $l \cdot s^{-1}$– 5 $l \cdot s^{-1}$even during the spring snowmelt. These were mostly diffuse inflows from fractured zones. When fault zones were breached, the inflows resembled heavy rainfall with a discharge of several $l \cdot s^{-1}$; however, they rapidly diminished after just a few days. Mihók and Jančura (2000) report average inflows into the Manó–Gabriela mine in the range of 2.0 $l \cdot s^{-1}$– 5.0 $l \cdot s^{-1}$, depending on the season and precipitation.

A cross-cut was driven from the Manó hereditary horizon along the northern edge of the Manó deposit, providing access to the siderite deposit at Kobeliarovo from the plant at Nižná Slaná (Jeleň et al., 1993). This 2,034 m long adit encountered water-filled fractures in crystalline limestones and rauvacs with discharge rates of 2 $l \cdot s^{-1}$– 3 $l \cdot s^{-1}$. Routine measurements of the outflow from the Transport Adit prior to the development of the Kobeliarovo deposit documented a flow rate of up to 21 $l \cdot s^{-1}$, averaging 12.4 $l \cdot s^{-1}$. During mining, the water was discharged to the surface at Nižná Slaná without flowing into the deeper levels of the Manó–Gabriela deposit/mine. It is likely that during the flooding of the mine, this flow was redirected into an unnamed shaft near the Manó II blind shaft and thus into the workings of the Manó–Gabriela mine.

Table 1 Average chemical composition of carbonates of the Manó – Gabriela deposit (source: Turan, Turanová, 1993).

Table 1 Average chemical composition of carbonates of the Manó – Gabriela deposit (source: Turan, Turanová, 1993).

	FeO	MgO	CaO	MnO	CO_2	n
Siderite – basic type	56.66	4.15	0.44	3.33	39.16	18*, 13**
Siderite – vein	53.54	6.54	2.79	0.70	39.94	13*, 8**
Siderite from black shales	44.34	5.67	0.45	9.79	39.79	11
Siderite from limestone deposits	50.88	5.19	1.10	3.17	39.66	10
Ankerite – basic type	16.73	10.79	28.12	2.12	44.28	43 (16 – MnO)
Ankerite from black shales	12.26	8.97	21.84	13.88	43.18	3
Calcite	53.72	0.02	1.61	0.92	43.73	20

Explanations: Arithmetic mean of the set in wt. %. The concentration of FeO, MgO and $_{CO_2}$was determined by the manometric method and converted to 100% carbonate (GÚ PriF UK Bratislava). The concentration of CaO and MnO was determined by the AAS method (GÚ PriF UK Bratislava).

Explanations: Arithmetic mean of the set in wt. %. The content of FeO, MgO and $_{CO_2}$was determined by the manometric method and converted to 100% carbonate (GÚ PriF UK Bratislava). The content of CaO and MnO was determined by the AAS method (GÚ PriF UK Bratislava).

Table 2 Average composition of black phyllites from the Manó–Gabriela deposit in Nižná Sláná (source: Turanová et al., 1995a).
Table 2 Average composition of black phyllites from the Manó–Gabriela deposit in Nižná Sláná (source: Turanová et al., 1995a).

SiO_2	Al_2O_3	Fe_2O_3 total	FeO	CaO	MgO	MnO	Na_2O	K_2O	TiO_2	Loss on ignition	Total	Corg.
wt. %												
56.31	9.98	7.02	n	7.73	2.43	0.78	0.19	2.37	0.47	12.66	1.32	1.26

Explanatory notes: Number of samples: 46. n – unspecified.

Table 3 Average concentration of metals and metalloids in black phyllites of the Manó – Gabriela deposit in Nižná Sláná (source: Turanová et al., 1995b).
Table 3 Average concentration of metals and metalloids in black phyllites of the Manó–Gabriela deposit in Nižná Sláná (source: Turanová et al., 1995b).

As	Cd	Co	Cr	Cu	Hg	Ni	Pb	Sb	V	Zn
(ppm)										
437.20	2.14	74.40	102.40	131.60	4.63	240.60	127.75	116.86	406.00	n

Explanatory notes: Number of samples: 10. n – unspecified.

The Nižná Slaná area has a snow-rain runoff regime with accumulation from November to February and high water levels from March to May (Miklós et al., 2002). The highest flows occur in April, the lowest in January–February and September–October. The average annual air temperature at the nearest weather station in Rožňava is 9.0 °C, for the reference period 1981–2010.

METHODOLOGY OF MEASUREMENTS AND THEIR INTERPRETATION

Sampling of mine water flowing through the Gabriela shaft into the Marta adit has been carried out monthly since the overflow was discovered in February 2022 as part of the state sub-monitoring system Geological Factors (ČMS GF) – the 'Impact of Mining on the Environment' (VŤŽP) subsystem, (www.geology.sk/ geoinfoportal; Bajtoš et al., 2023, 2024, 2025) and as part of the monitoring carried out in connection with the declaration of a state of emergency on the River Slaná. Samples were taken directly at the spillway from the Gabriela pit. In the field, portable WTW series field instruments were used to determine pH, water temperature and air temperature, specific electrical conductivity of water, dissolved $O_2$and redox potential (E_H). The $E_H$value measured using an Ag/AgCl probe was converted to a standard hydrogen electrode.

Samples of mine water were collected in polyethylene bottles. Samples for the determination of trace elements were filtered through 1 µm paper filters upon collection and subsequently through 0.45 µm membrane filters in the laboratory, and were preserved with concentrated HNO_3(0.5 ml / 100 ml). All samples were analysed using standard laboratory procedures in an accredited geoanalytical laboratory ŠGÚDŠ RC Spišská Nová Ves (www.geology.sk). Concentrations of Fe, Na, K, Ca, Mg, Mn, Al, Co, Ni and Zn were measured using the AES-ICP method with an AGILENT TECHNOLOGIES 5110 instrument. As concentrations were measured using the ICP-MS method with an AGILENT TECHNOLOGIES 7900 instrument. The concentration of $SO_4^{2-}$was measured by ion chromatography using a DIONEX ICS 5000 instrument. The concentration of $HCO_3^-$was determined by calculation from electrochemical measurements.

The instantaneous discharge rate of mine water was also measured during all sampling operations. These measurements were initially carried out using a Valeport Model 801 electromagnetic flowmeter in the discharge channel; later – following the construction of a measuring weir – by the volumetric method, using a calibrated container and a stopwatch. Flow measurements in the open channel were carried out using the point method in accordance with ON 73 6571.

We evaluated the temporal changes in the concentrations of the monitored elements in the mine water of the Gabriela shaft using standard statistical methods in the MS EXCEL and STATISTICA software environments (STATISTICA Cz 10, StatSoft Inc.). When creating data sets for statistical calculations, we replaced the results of laboratory measurements where element concentrations were below the detection limit of the relevant measurement method with half the value of the limit of quantification. We monitored the occurrence of outliers, as well as the nature of the distribution of values in the datasets, visually on histograms. When assessing the nature of the distribution of values in the datasets based on kurtosis and skewness, we considered values in the range from -0.5 to 0.5 as an indication of probable

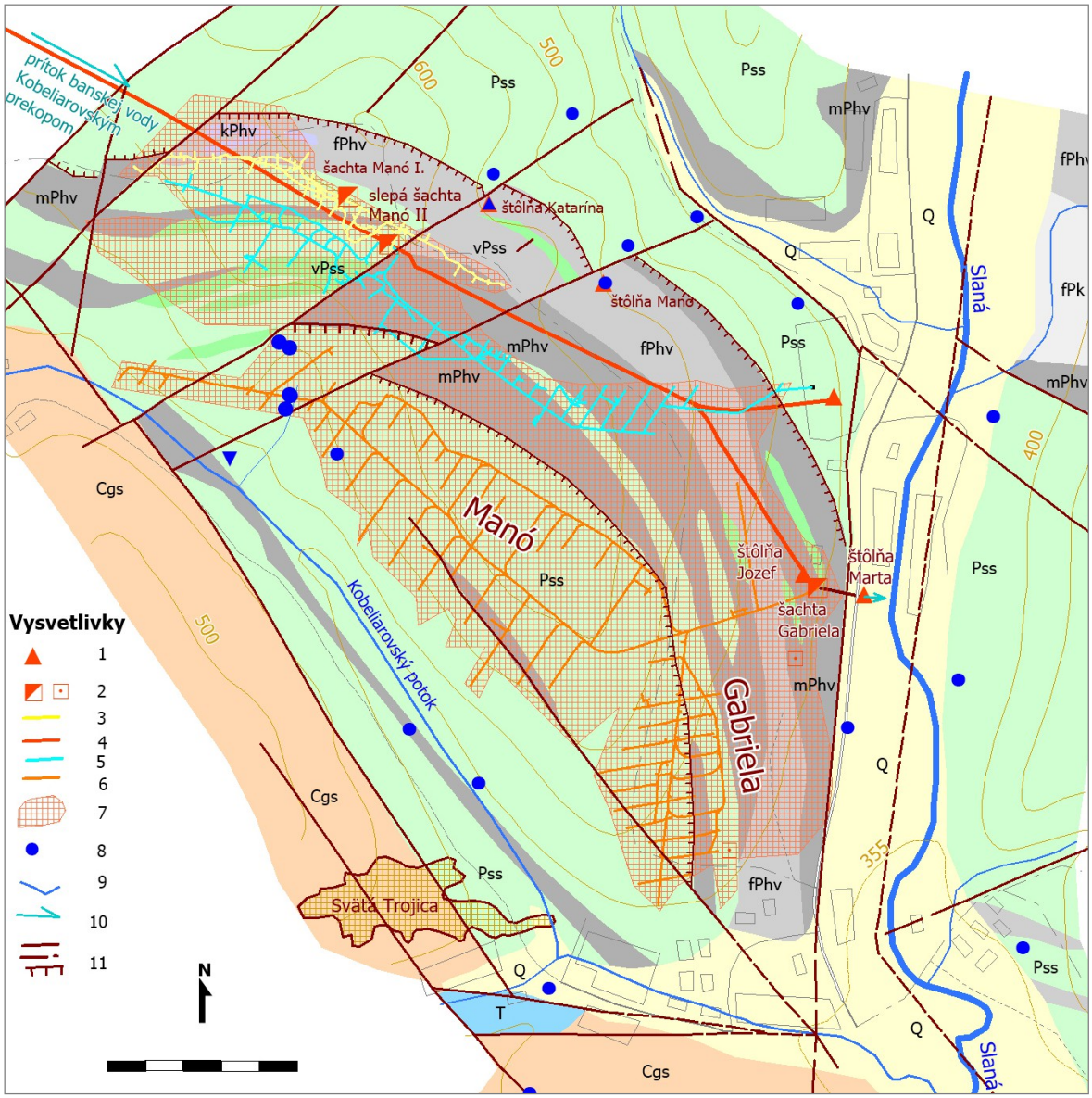

Fig. 1 Geological map of the Manó – Gabriela mine area.
Legend: 1 – adit mouth, 2 – shaft, chimney, 3 – galleries of the third level (483 m a.s.l.), 3 – galleries of the sixth level (395 m a.s.l.), 5 – galleries of the seventh level (355 m a.s.l.), 6 – galleries of the 11th level (249 m a.s.l.), 7 – extent of underground mining works, 8 – spring, 9 – surface stream, 10 – mine water flow, 11 – fault, covered fault, thrust fault. The galleries of Horizons IV, V, VIII, X and XII are not shown in the diagram to improve clarity. Codes for rock units exposed at the surface of the area, shown by colour in the map (compiled from 1:25,000 scale geological maps in Grecula et al., 2009): Q – fluvial and proluvial sediments, Quaternary; T – carbonates, Triassic; Cgs – conglomerates, sandstones and shales, Gočaltov Group – Carboniferous; Pss – phyllites and recrystallised phyllites of the Smolník Formation, Early Palaeozoic; vPss – recrystallised rocks of keratophyre volcanism of the Smolník Formation, Early Palaeozoic; kPhv – carbonates, Holecká layers of the Betliar Formation, Early Palaeozoic; fPhv – recrystallised black pelitic phyllites with intercalations of lydites, carbonates and volcanic rocks, Holecká layers of the Betliar Formation, Early Palaeozoic; mPhv – recrystallised black pelitic phyllites, Holecká layers of the Betliar Formation, Early Palaeozoic.

Fig. 1 Geological map of the Manó – Gabriela mine.
1 – adit mouth, 2 – shaft, 3 – mine corridors of the third level (483 m a.s.l.), 4 – mine corridors of the sixth level (395 m a.s.l.), 5 – mine galleries of the 7th level (355 m a.s.l.), mine galleries of the 11th level (249 m a.s.l.), 7 – spatial extent of underground mine workings, 8 – spring, 9 – surface watercourse, 10 – mine water flow, 11 – fault, concealed fault, thrust fault. The drifts of the IVth, Vth, VIIIth, Xth, and XIIth levels are not shown in the diagram for greater clarity. Codes of lithological units outcropping at the surface of the area, indicated by colours (compiled according to geological maps at a scale of 1:25 000 in Grecula et al., 2009): Q – fluvial and proluvial sediments, Quaternary; T – carbonates, Triassic; Cgs – conglomerates, sandstones, and shales, Gočaltovská Group – Carboniferous; Pss – phyllites and recrystallised phyllites of the Smolník Formation, Lower Palaeozoic; vPss – recrystallised rocks of keratophyre volcanism of the Smolník Formation, Lower Palaeozoic; kPhv – carbonates, Holec Beds of the Betliar Formation, Lower Palaeozoic; fPhv – recrystallised black pelitic phyllites with intercalations of lydite, carbonates, and volcanic rocks, Holec Beds of the Betliar Formation, Lower Palaeozoic; mPhv – recrystallised black pelitic phyllites, Holec Beds of the Betliar Formation, Lower Palaeozoic.

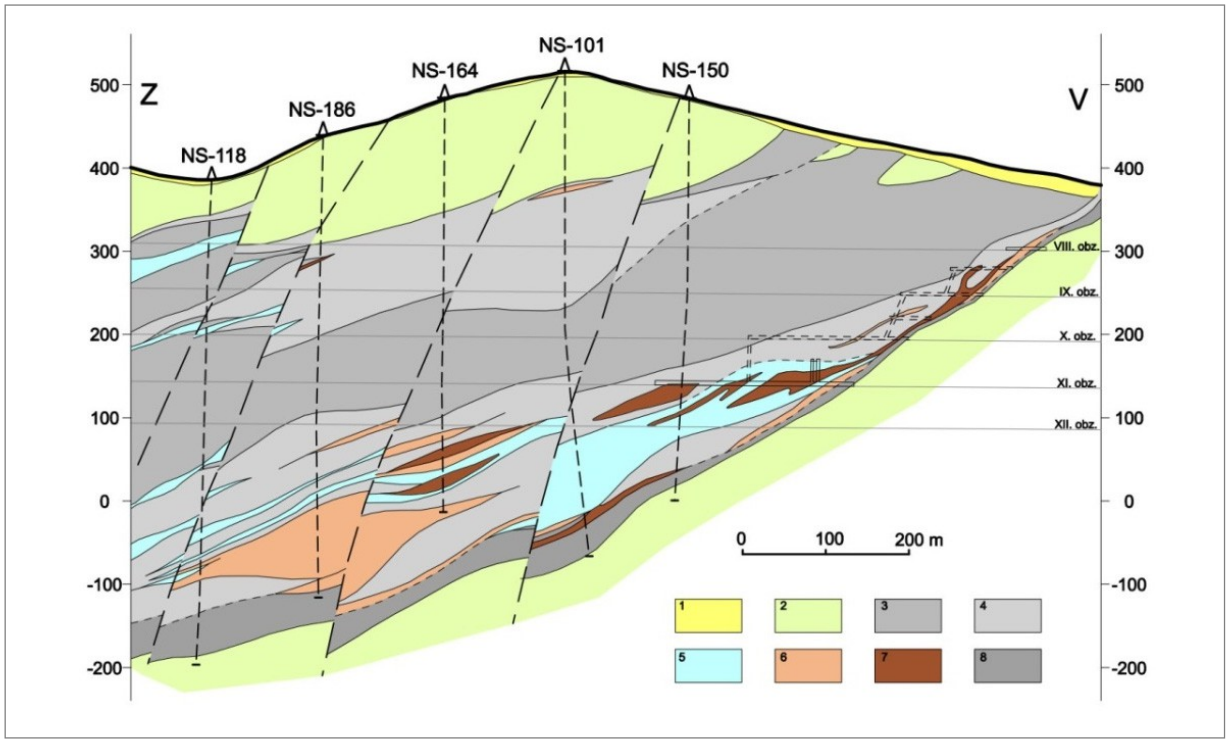

Fig. 2 Cross-section through the eastern part of the Manó–Gabriela deposit (Mihók in Grecula et al., 1995).
Legend: 1 – Quaternary slope sediments – scree, 2 – metaryolite tuffs, 3 – grey and black phyllites, 4 – black phyllites with lydite intercalations, 5 – metamorphosed limestone, 6 – ankerite, 7 – siderite, 8 – underlying sericitic phyllite.
Fig. 2 Geological cross-section through the Manó – Gabriela siderite deposit.
Explanations: 1 – Quaternary sediments, 2 – tuffs, 3 – black and grey phyllites, 4 – black phyllite with interlayers of lyddite, 5 – crystalline limestone, 6 – ankerite, 7 – siderite, 8 – sericitic phyllite. The cross-section is oriented in a west (left) – east (right) direction.

normal distribution, with values less than -2 and greater than 2 indicating a significant deviation from normality. The remaining values are considered an indicator of a slight deviation from normality.

The PHREEQC computer program (Parkhurst, Appelo, 2013), designed for a wide range of hydrogeochemical calculations – simulations of chemical reactions and the transport of substances in low-temperature aqueous solutions – was used for the hydrogeochemical assessment. Using this, we calculated the saturation indices *(SI)* of the aqueous solution with respect to selected minerals and gases and identified the forms of occurrence of the monitored elements (species) present in the aqueous solution. The aforementioned types of calculations, also known as speciation calculations, are performed in the SOLUTION program module. Based on the results of chemical water analyses, the programme block calculates the molar quantities of species and the values of *SI* saturation indices (or non-equilibrium indices according to Hanzel et al., 1998) of the water with respect to minerals and gases, using an ion association model. *SI* values indicate the state of saturation of the solution with respect to the mineral: *SI* values close to zero indicate equilibrium, negative values indicate undersaturation of the solution with respect to the mineral, and positive values indicate its supersaturation. With regard to

Based on current knowledge of the variability in the chemical composition of the carbonates in the deposit under study (Turan, Turanová, 1993; Table 1), the following average composition of the locally specific ore carbonates is assumed: siderite from stratiform deposits – $Fe_{0.892}Mg_{0.050}$ $Ca_{0.006}$ $Mn_{0.052}$ CO_3 (siderite-B), vein siderite – $Fe_{0.869}$ $Mg_{0.08}$ $Ca_{0.04}$ $Mn_{0.011}$ CO_3 (siderite-V), siderite in black shales – $Fe_{0.774}$ $Mg_{0.068}Ca_{0.006}$ $Mn_{0.152}$ CO_3 (siderite-BS), ankerite in stratiform deposits – $Ca_{1.00}$ $(Fe_{0.676}$ $Mg_{0.26}Mn_{0.064}$ $(CO_3)_2$ (ankerite-B), ankerite in black shales – $Ca_{1.00}$ $(Fe_{0.544}Mg_{0.216}$ $Mn_{0.24}$ $(CO_3)_2$ (ankerite-BS) and calcite $Ca_{0.892}$ $Mg_{0.076}$ $Mn_{0.016}$ CO_3 in stratiform deposits (calcite-B). We determined the SI values for the identified siderite and calcite modifications by calculation from the SI values of the end members of the solid solution according to their relative proportions (siderite, magnesite, calcite and rhodochrosite – SI values from the PHREEQC database).

In the calculations of the saturation state with respect to the solid solution $CaCu(_{AsO_4})(OH)$, olivine and weilite, the *logK* values reported by Gasková (in Bhattacharya et al., 2007) were used: 1.29, 2.39 and 2.36. In the calculations, we used input data from laboratory analyses and the corresponding

pH and E_H /*pe* values, measured at the time of sampling.

RESULTS

Temporal evolution of the concentration of monitored elements in the mine water of the Gabriela shaft

When evaluating the temporal evolution of the chemical composition of mine water flowing out of the Gabriela shaft, it is necessary to take into account the impact of significant changes in the mine's water circulation regime. The first such event was the restoration of the continuous outflow of water flowing through the Kobeliarovský adit via the Manó heritage horizon to the surface, or rather the prevention of its inflow through the chimney at the Manó II blind shaft into the mine workings at the Manó–Gabriela deposit, by means of technical intervention in the mine. This was carried out in June 2022 and, as a result, the volume of water flowing out through the Gabriela shaft decreased from approximately 20 $l \cdot s^{-1}$ to 2 $l \cdot s^{-1}$ – 3 $l \cdot s^{-1}$. Another artificial intervention in the mine's hydraulic regime was the pumping of water at a rate of approximately 3 $l \cdot s^{-1}$ from the drainage channel of the Manó heritage horizon, carried out between 26 August and 30 September 2022, as a result of which no water flowed through the Gabriela shaft during that period. A significant change in flow conditions within the mine is also indicated by the sharp rise in the temperature of the water flowing out through the Gabriela shaft from 18 °C to 34 °C, which was recorded between 30 July to 31 August 2023. This was likely caused by the development of leaks in the dam and the re-entry of part of the water flowing through the Kobeliarovský adit towards the Jozef adit into the mining areas of the Manó–Gabriela deposit. As pumping water from the sinkhole had no significant effect on the temperature, specific electrical conductivity or chemical composition of the water flowing out of the Gabriela shaft, it is appropriate to distinguish between the following time periods in the assessment: (1) the initial period, lasting from the discovery of the outflow until the prevention of water inflow from the Kobeliarovský tunnel into the mining areas of the Manó–Gabriela deposit (February 2022 – June 2022); (2) the second period, lasting from the prevention of water ingress from the Kobeliarovský adit into the mining areas of the Manó–Gabriela deposit until the onset of a sharp rise in the temperature of the water flowing out of the Gabriela shaft (July 2022 – July 2023) and (3) the subsequent final period (Table 4).

The outflow from the Gabriela shaft likely occurred 10 February 2022. Initially, it was low in mineralisation (on 14 February 2022 EC = 21.6 $mS \cdot m^{-1}$), the water had a slightly alkaline reaction and a temperature corresponding to the average annual temperature of the site. In the following period, however, both the mineralisation and the water temperature rose continuously (Fig. 3). On 24 February 2022, an EC value of of 2070 $mS \cdot m^{-1}$ and a water temperature of 16.5 °C. On 10 March 2022, the EC value reached 2450 $mS \cdot m^{-1}$ and the water temperature 31 °C, and in the subsequent period up to 9 June 2022 (when technical intervention prevented the inflow of water from the Kobeliarovský adit to the Manó–Gabriela mine, and its outflow through the hereditary horizon into the Jozef adit was restored) After reaching a maximum of 26.8 $mS \cdot m^{-1}$, the EC fell to 23 $mS \cdot m^{-1}$, and the water temperature fluctuated between 35 °C and 36 °C. The water's pH fell into the acidic range (pH = 5.0–5.5). The concentration of sulphate anions during this period rose to 40 $g \cdot l^{-1}$, magnesium to 30 $g \cdot l^{-1}$ – 35 $g \cdot l^{-1}$ (Fig. 4), iron to 5 $g \cdot l^{-1}$ and manganese to 0.6 $g \cdot l^{-1}$ (Fig. 5). Concentrations of calcium, potassium and sodium also rose significantly (Fig. 6). Arsenic concentrations reached 17 $mg \cdot l^{-1}$, nickel exceeded 20 $mg \cdot l^{-1}$ (Fig. 7), whilst zinc, cobalt and aluminium approached the 5 $mg \cdot l^{-1}$ level (Fig. 8).

Following the diversion of the Kobeliarovský canal away from the deep workings of the Manó–Gabriela mine, the temperature of the water flowing from the Gabriela shaft dropped to 17 °C–18 °C (9 November 2022), where it stabilised. EC during this period fell to a level of 2000 $mS \cdot m^{-1}$ – 2100 $mS \cdot m^{-1}$. The concentration of SO_4^{2-} gradually stabilised at a level of approximately 25 $g \cdot l^{-1}$ and Mg at a level of 4 $g \cdot l^{-1}$. The trend of a steady decline in the concentrations of Fe, Mn and Ni from the previous period persisted, whilst the concentration of As rose from 8 to 12 $mg \cdot l^{-1}$.

The final phase of the assessment period began at the end of July 2023, when the water temperature rose significantly, reaching 33.6 °C on 24 August 2022 and stabilising at around 35 °C from 15 September 2023. During this rise in water temperature, the EC rose synchronously to approximately 2500 $mS \cdot m^{-1}$. The water's reaction did not change significantly. Following an initial sharp increase in the concentrations of SO^{2-} and Mg, their trend took on a downward character – this can be described by the equations SO^{2-} ($mg \cdot l^{-1}$) = $-9.802t + 34095$ ($R^2 = 0.765$, R = 0.874) and Mg ($mg \cdot l^{-1}$) = $-1.933t + 7402$ ($R^2 = 0.464$, R = 0.681), where *t* is the day number from the start of the evaluated time period set at 7 June 2022. The downward trend in iron and manganese concentrations observed in previous time periods was maintained in the final period, reaching levels of 1.8 $g \cdot l^{-1}$ and 0.2 $g \cdot l^{-1}$ respectively by the end of 2024. This decline can be described for iron over the entire assessed period (from 7 June 2022) by the exponential regression equation Fe ($mg \cdot l^{-1}$) $= 4242e^{-0.001t}$ (coefficient of determination $R^2 = 0.89$), The decline in manganese concentration can be expressed by the exponential regression equation Mn ($mg \cdot l^{-1}$) = $579.64e^{-0.001t}$ (coefficient of determination $R^2 = 0.93$) with a similarly defined parameter *t*. The concentration of Ni stabilised at 5 $mg \cdot l^{-1}$ in the final time period, whilst that of As fluctuated irregularly between 15 $mg \cdot l^{-1}$ and 23 $mg \cdot l^{-1}$. The calcium concentration fluctuated steadily around 0.45 $g \cdot l^{-1}$ (as in the previous time period), whilst those of potassium and sodium remained relatively stable. In contrast, zinc and aluminium concentrations were relatively stable, whilst Co showed a slight upward trend (Fig. 8).

Table 4 Concentrations of risk elements in the discharge from the Gabriela shaft.
Table 4 The concentration of risk elements in the effluent from the Gabriela shaft.

Date sampling	Q ($l \cdot s^{-1}$)	Tvo (°C)	EC ($mS \cdot m^{-1}$)	pH (-)	so_4^{2-}	Fe	Mn	Zn	As	Ni ($mg \cdot l^{-1}$)	Co	Al	Mg	Ca	Na	K	HCO_3^-
14 February 22	4.49	7.7	21.6	7.93	50.3	0.145	0.174	0.029	0.00025	0.002	0.004	0.05	15.4	21.2	-	-	-
24 Feb 22	11.4	16.5	**2070**	**5.78**	25,936	2950	383	1.33	**4.154**	**18.4**	**3.25**	**1.16**	5,100	306	31	82	82
10 March 22	14.2	30.9	**2,450**	**5.53**	37,500	4020	527	2.03	**10.041**	**19.3**	**0.451**	0.01	6130	302	-	-	-
24 March 22	16.8	35.5	**2,500**	**5.02**	30,088	4410	566	2.68	**15.422**	**22.6**	**2.71**	0.02	6090	310	-	-	-
5 April 22	18.5	36.1	**2480**	**5.06**	34,108	5020	592	2.76	**16.763**	**23.4**	**3.1**	**3.81**	7,110	316	-	-	-
21 April 22	18.8	36.6	**2580**	**5.31**	35,496	5103	517	2.71	**17.200**	**10.76**	**1.603**	**2.57**	7,207	504	35	165	165
18 May 22	18.4	34.1	**2330**	**5.30**	37,100	4640	634	3.11	**14.703**	**19.7**	**0.888**	**4.13**	6,220	313	32	121	121
31 May 22	19.4	35.2	**2260**	**5.06**	36,400	4530	663	4.38	**16.399**	**21.1**	**3**	**4.60**	5,950	461	-	-	-
8 June 22	21.3	34.9	**2310**	**5.22**	41,078	4880	734	4.40	**17.175**	**21.3**	**1.54**	**4.42**	6,160	458	-	-	-
23 June 22	2.84	29.4	**2310**	**5.56**	39,480	4120	607	3.54	**14.026**	**20.2**	**1.88**	**3.59**	5,990	442	32	102	102
3 August 22	2.61	23.3	**2330**	**5.17**	26,450	4030	567	2.59	**12.635**	**23.4**	**2.89**	**3.19**	4,710	318	28	84	84
9 August 22	2.27	22.7	**2020**	**5.31**	25,800	4,240	562	3.43	**11.929**	**19.5**	**1.34**	**3.34**	5030	438	25	90	90
15 August 22	1.05	22.1	**2130**	**5.32**	33,750	4260	592	2.46	**12.316**	**24.3**	**3.6**	**3.22**	4,970	314	31	85	85
12 September 22	0*	19.2	**2060**	**5.42**	30,000	3,600	480	2.13	**8.989**	**20.4**	**2.9**	**2.48**	4,510	344	27	75	75
11 Oct 22	1.65	18.5	**2060**	**5.30**	27,599	3460	460	1.80	**8.324**	**15.9**	**2.38**	**2.16**	4,740	311	26	71	71
9 Nov 22	1.35	17.1	**2070**	**5.46**	30,000	3,220	420	2.55	**8.060**	**17.6**	**2.02**	**2.1**	4,280	448	30	74	74
15 Dec 22	0.93	17.1	**2090**	**5.28**	31,500	3640	461	2.83	**7.815**	**17.9**	**2.74**	**2.74**	4,860	499	41	96	96
16 Jan 23	2.86	17.1	**2040**	**5.29**	26,188	3310	432	2.87	**12.137**	**15.5**	**0.91**	**2.41**	3,830	469	28	87	87
14 Feb 23	1.92	16.7	**2000**	**5.28**	25,532	3,340	433	3.19	**11.400**	**14.5**	**1.29**	**2.74**	3,870	477	31	107	107
20 March 23	2.56	17.2	**2000**	**5.21**	25,720	3,270	388	2.59	**11.700**	**12.2**	**1.11**	**2.52**	3,740	446	24	93	93
17 April 23	1.13	17	**2040**	**5.33**	26,720	3,270	409	2.53	**11.897**	**11.6**	**0.727**	**2.35**	3,850	467	26	96	96
18 May 23	0.79	17.3	**2050**	**5.42**	24,098	3000	376	2.19	**10.500**	**10**	**0.485**	**2.21**	3,790	451	30	109	109
13 June 23	2.33	17.8	**2070**	**5.43**	28,609	3040	375	2.26	**11.714**	**9.62**	**0.493**	**2.14**	3,830	456	28	108	108
11 July 23	2.61	18.2	**2100**	**5.38**	24,800	3050	309	2.14	**14.600**	**9.11**	**0.434**	**2.36**	4,580	465	36	141	141
14 August 23	2.45	31.8	**2,400**	**5.18**	30,276	2570	298	1,100	**18,630**	**6.47**	**0.297**	**1.45**	6,090	491	47	155	155
12 September 23	2.89	35.4	**2,490**	**5.20**	29,302	2350	277	0.889	**18.542**	**5.64**	**0.2**	**1.42**	6,350	481	51	166	166
10 Oct 23	2.51	35.5	**2370**	**5.19**	29,283	2340	260	0.561	**19.869**	**2.78**	0.114	**1.03**	6,520	385	44	152	152
13 Nov 23	2.15	33.5	**2410**	**5.13**	28,464	1820	245	0.864	**19.791**	**5.19**	**0.262**	**1.57**	6,300	476	56	162	162
19 Dec 23	3.22	36.1	**2370**	**5.12**	29,700	2410	262	0.797	**19.200**	**5.44**	**0.263**	**1.34**	7,110	522	56	176	176
25 Jan 24	5.39	37.6	**2,400**	**5.13**	29,500	2190	234	0.664	**20.600**	**5.06**	**0.38**	**1.56**	6,500	480	53	169	169
26 Feb 24	5.12	37.4	**2380**	**5.22**	26,670	2130	231	0.025	**20.194**	**4.99**	**0.465**	**1.58**	6,410	461	49	142	142
26 March 24	4.68	36.9	**2410**	**5.32**	26,900	1890	208	0.635	**17.700**	**4.92**	**0.523**	**1.12**	5,830	453	52	143	143
24 April 24	5.87	36.7	**2480**	**5.21**	24,733	2020	218	0.647	**16.704**	**5.08**	**0.515**	**1.41**	5,950	459	49	149	149
23 May 24	4.12	36.1	**2270**	**5.20**	26,800	1990	217	0.685	**16.700**	**5.28**	**0.437**	**1.48**	6,100	474	51	168	168
13 June 24	4.53	36.1	**2270**	**5.20**	25,019	1800	201	0.696	**17.100**	**4.95**	**0.421**	**1.1**	5,470	449	65	174	174
18 July 24	4.53	34.9	**2210**	**5.36**	27,577	1360	241	0.785	**19.100**	**5.92**	**0.62**	**1.4**	6,340	485	51	159	159
14 August 24	4.54	35.5	**2230**	**5.52**	27,228	2130	232	0.512	**22.494**	**3.43**	**0.341**	**0.96**	7070	356	46	128	128
30 September 24	4.26	34.1	**2140**	**5.28**	25,163	1950	211	0.707	**14.698**	**5.49**	**0.433**	**1.23**	5,530	464	47	167	167
24 Oct 24	4.25	33.3	**2100**	**5.35**	25,874	1950	212	0.696	**18.923**	**5.52**	**0.811**	**1.35**	5,890	486	60	231	231
19 Nov 24	4.28	34.0	**2120**	**5.34**	25,351	1810	199	0.611	**18.824**	**5.24**	**0.576**	**1.14**	5,700	503	46	132	132
17 Dec 24	2.82	34.6	**2120**	**5.45**	25,309	1780	190	0.556	**18.761**	**4.92**	**0.483**	**0.94**	5,410	444	45	129	129
IT criterion	-	-	*300*	*< 6*	-	-	-	*5*	*0.1*	*0.2*	*0.2*	*0.40*	-	-			-

Explanations: Values exceeding the IT criteria (Directive of the Ministry of the Environment of the Slovak Republic No. 1/2015 – 7) for groundwater are shaded.
Explanations: Values exceeding the IT criteria (Directive of the Ministry of the Environment of the Slovak Republic No. 1/2015 – 7) for groundwater are shaded.

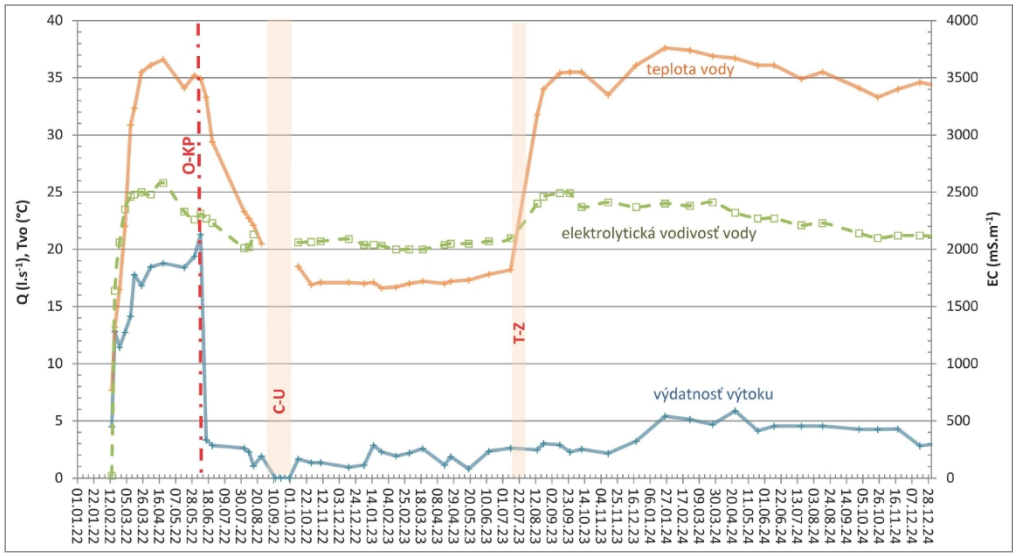

Fig. 3 Temporal development of water temperature (Tvo) and electrical conductivity (EC) and the discharge rate from the Gabriela shaft from the time the outflow was discovered until the end of 2024. Explanatory notes: O-KP – period of diversion of the Kobeliarovský tunnel water flow away from the deep mining operations below the Manó water-bearing horizon; C-U – period of water extraction from the Manó–Gabriela mine via a drain from the Manó water-bearing horizon; TZ – start of a significant rise in the water temperature of the Gabriela shaft.

Fig. 3 Time evolution of temperature (Tvo) and electrolytic conductivity (EC) of water and the yield of the overflow from the Gabriela shaft in the period from the appearance of the outflow to the end of 2024. Explanations: O-KP – time of prevention of water inflow from the Kobeliarovský corridor to the Manó – Gabriela mine, C-U – time of pumping water from the Manó – Gabriela mine via the decaying corridor, TZ – beginning of a significant increase in the temperature of the Gabriela shaft water.

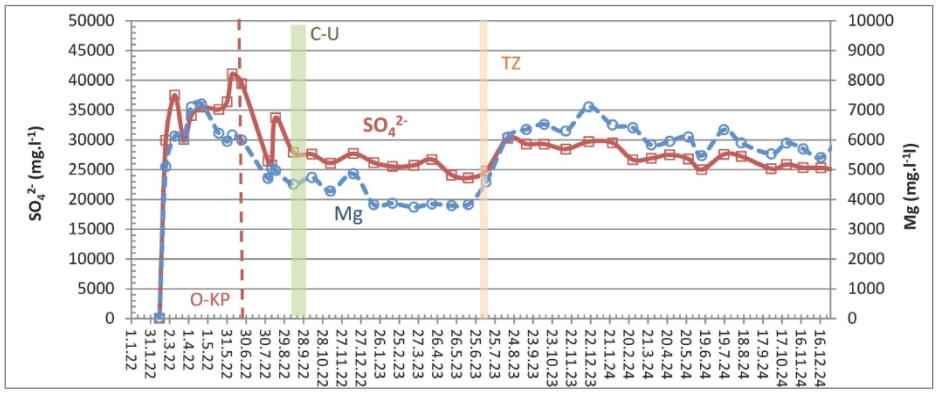

Fig. 4 Time evolution of the concentration of sulphate anion and magnesium in the mine water of the Gabriela shaft in the period from the appearance of the outflow to the end of 2024. Explanations as for Fig. 3.

Fig. 4 Time evolution of the concentration of sulphate anion and magnesium in the mine water of the Gabriela shaft in the period from the appearance of the outflow to the end of 2024. Explanations as for Fig. 3.

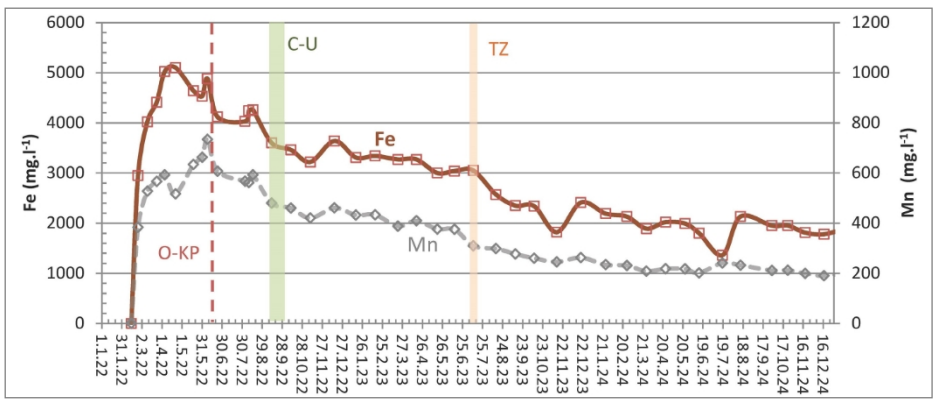

Fig. 5 Time evolution of iron and manganese concentrations in the mine water of the Gabriela shaft from the appearance of the outflow to the end of 2024. Explanations as for Fig. 3.

Fig. 5 Time evolution of iron and manganese concentrations in the mine water of the Gabriela shaft from the appearance of the outflow to the end of 2024. Explanations as for Fig. 3.

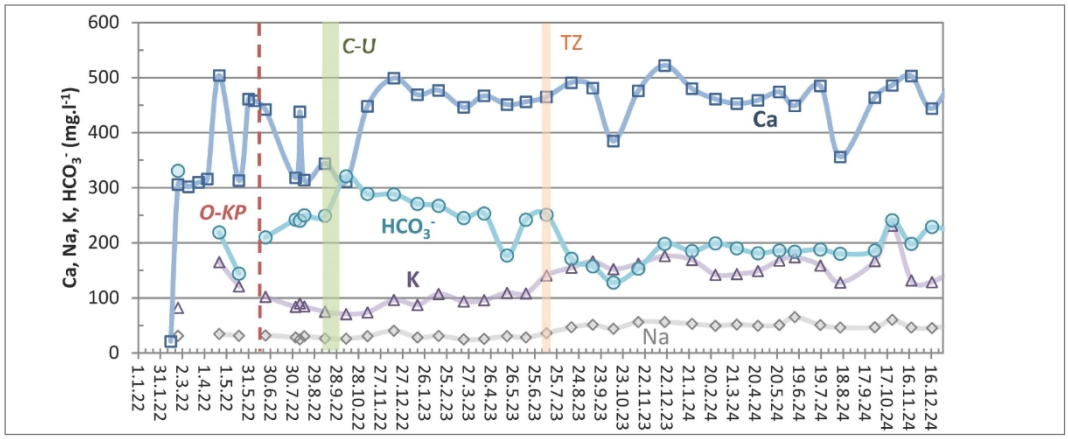

Fig. 6 Time evolution of the concentration of calcium, magnesium and sodium in the mine water of the Gabriela shaft in the period from the appearance of the outflow to the end of 2024. Explanations as for Fig. 3.
Fig. 6 Time evolution of the concentration of calcium, magnesium and sodium in the mine water of the Gabriela shaft in the period from the appearance of the outflow to the end of 2024. Explanations as for Fig. 3.

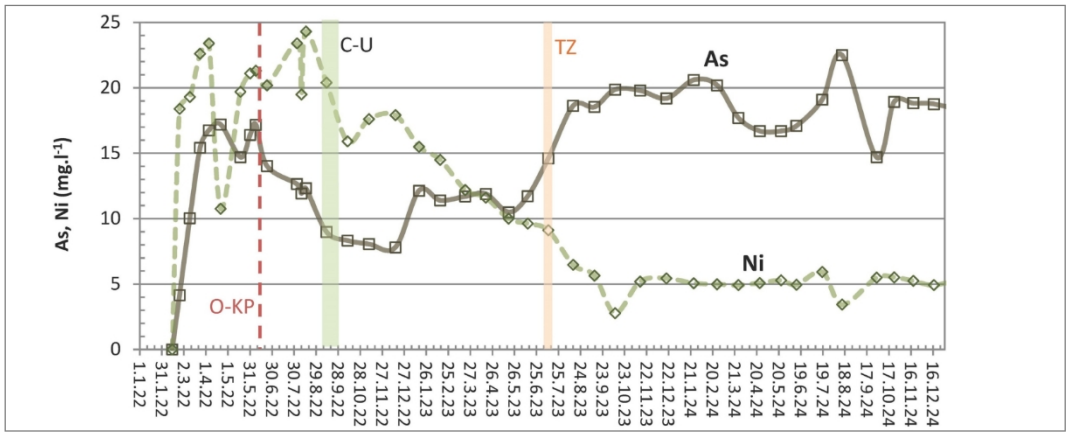

Fig. 7 Time evolution of the concentration of arsenic and nickel in the mine water of the Gabriela shaft from the appearance of the outflow to the end of 2024. Explanations as for Fig. 3.
Fig. 7 Time evolution of arsenic and nickel concentrations in the mine water of the Gabriela shaft from the appearance of the outflow to the end of 2024. Explanations as for Fig. 3.

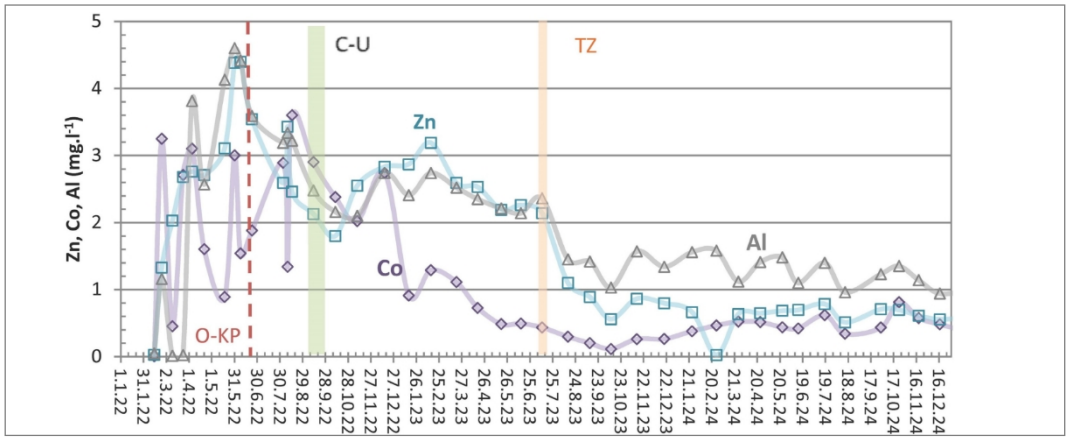

Fig. 8 Time evolution of zinc, cobalt and aluminium concentrations in the mine water of the Gabriela shaft from the appearance of the outflow to the end of 2024. Explanations as for Fig. 3.
Fig. 8 Time evolution of zinc, cobalt and aluminium concentrations in the mine water of the Gabriela shaft from the appearance of the outflow to the end of 2024. Explanations as for Fig. 3.

Hydrogeochemical characteristics of the water flowing out of the Gabriela shaft

The water flowing out of the Gabriela shaft is acidic; in the first sample of highly mineralised water from 24 February 2022, the pH value was 5.78 and subsequently fluctuated within the range of pH = 5.12 – 5.56. In the cationic fraction of the chemical composition, magnesium predominates (66 wt% – 86 wt%, average 75 wt%) over iron (8 wt% – 25 wt%, average 18 wt%), with significant contributions from calcium (2.2 wt% – 4.9 wt%, average 3.8 wt%) and manganese (1.3 wt% – 3.6 wt%, average 2.2 wt%), whilst the proportion of sodium or potassium does not exceed 1 wt%. In the anionic range, sulphates are absolutely dominant (98.8 wt% – 99.5 wt%), whilst the proportion of bicarbonates is only 0.3 wt% – 0.9 wt%). The total mineralisation of the water in these samples was 31.8 $^{g\cdot l^{-1}}$and 49.$^{4\ g\cdot l^{-1}}$ respectively, with an average of 37.3 $^{g\cdot l^{-1}}$. The measured $E_H$values range from 177 mV to 433 mV with an average of 221 mV (corresponding to values *of pe* = 3.6 – 4.4 with an average of 3.8), thus falling within the range characteristic of anoxic to weakly aerobic conditions. The concentration of oxygen dissolved in water ranges in the hundredths $^{of\ mg\cdot l^{-1}}$, representing a saturation of 1%. The macrochemical composition of the water – or rather the proportion of the main components of water mineralisation – did not change significantly during the period under review (Fig. 9).

Statistical evaluation of the monitored parameters

The basic statistical parameters of the sets of measured values for the three selected time periods of the assessed period are given in Table 5.

The relative variability of the data in the evaluated sets is lowest for pH, where it did not exceed 0.1 in periods II and III. It is relatively low (less than 0.7) in these periods for sulphates, iron, manganese and arsenic.

The calculated values of skewness and kurtosis, ranging from -0.5 to 0.5, suggest a normal distribution only in the datasets for zinc from period I, pH from period II and magnesium from period III. In several cases, normality is indicated by the skewness value, but the kurtosis value lies outside the interval indicating normality. In the case of slight deviations from normality, positive skewness values predominate, indicating a probable positive (right-skewed) distribution. A slight negative (left-skewed) skewness is identified by a negative skewness value for Q, Tvo, Mn, As, Ni and Ca in period I, for Ca in period II, and for Tvo, Zn, Ni and Ca in period III. A significant deviation from normality can be assumed for the sets of parameters EC, pH, SO^{2-} , Fe and Mg from period I. Of the measurements listed in Table 4, only the As concentration in the sample from 14 February 2022 was below the detection limit.

Given the nature of the distribution of the evaluated data sets, it is appropriate to test the interrelationship of the evaluated parameters using Spearman's correlation. The results of this analysis, based on data for mine water discharge from the Gabriela shaft for the period 9 June 2022 – 31 December 2024, are shown in Table 6. The concentration of manganese, iron, nickel and zinc correlates most closely with the time elapsed since the start of this period *t*, and this correlation is negative. The concentration of arsenic shows the strongest positive correlation with it. The correlation between time *t* and discharge rate Q is also relatively strong. Of the elements monitored, Fe, Mn, Ni and Zn show the strongest mutual positive correlation. The strength of the positive correlation between magnesium and arsenic is also high. Water temperature, As, Mg and EC concentrations correlate positively with the discharge rate of mine water *Q* corresponding to the sampling period, whilst Mn, Ni, Fe, Zn and Co correlate negatively with it in a statistically significant manner.

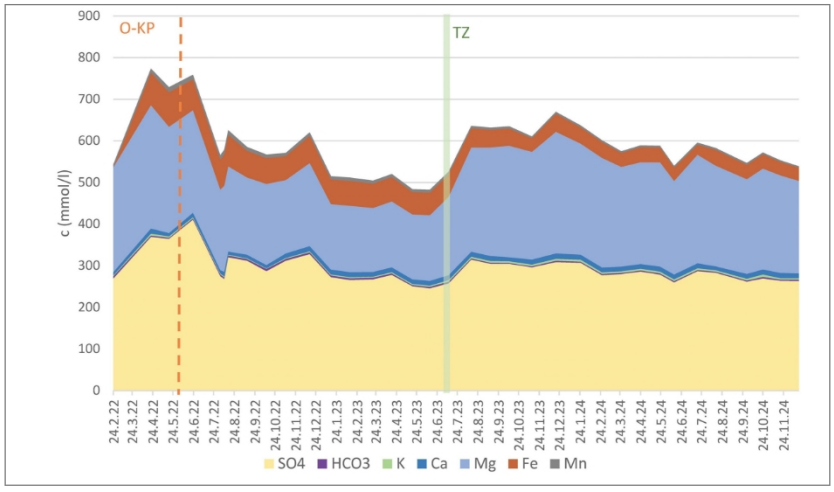

Fig. 9 Time evolution of the ratio of the mass of the main dissolved substances in the water flowing out of the Gabriela shaft. Explanations as for Fig. 3.

Fig. 9 Time evolution of the ratio of the mass of the main dissolved substances in the water flowing out of the Gabriela shaft. Explanations as for Fig. 3.

Table 5 Basic statistical parameters of the main physicochemical parameters of water and the concentration of risk elements dissolved in the water of the Gabriela shaft for selected sections of the evaluated period.
Table 5 Basic statistical parameters of the basic physicochemical parameters of the water and the concentration of risk elements dissolved in the water of the Gabriela shaft for selected sections of the evaluation period.

Year	Stat. parameter	Q ($l \cdot s^{-1}$)	Tvo (°C)	EC ($m \cdot m^{-1}$)	pH (-)	SO_4^{2-} ($mg \cdot l^{-1}$)	Fe ($mg \cdot l^{-1}$)	Mn ($mg \cdot l^{-1}$)	Zn ($mg \cdot l^{-1}$)	As ($mg \cdot l^{-1}$)	Ni ($mg \cdot l^{-1}$)	Co ($mg \cdot l^{-1}$)	Mg ($mg \cdot l^{-1}$)	Ca ($mg \cdot l^{-1}$)
II. 2022 – June 2022	min.	4.49	7.7	22	5.02	50	0.15	0.17	0.03	0.0003	0.002	0.004	15	21
	median	18.40	34.9	2330	5.30	35,496	4,530	566	2.71	15.42	19.70	1.60	6,130	313
period	max.	21.31	36.6	2580	7.93	41,078	5,103	734	4.40	17.20	23.40	3.25	7,207	504
I.	average	15.91	29.7	2111	5.58	30,862	3,950	513	2.60	12.43	17.40	1.84	5,554	332
	standard deviation	5.20	10.4	798	0.92	12,371	1,619	217	1.38	6.35	7.49	1.23	2,169	142
	rel. var.	0.91	0.83	1.10	0.55	1.16	1.13	1.30	1.61	1.12	1.19	2.02	1.17	1.54
	pointiness	2.22	1.77	8.07	7.20	5.93	5.12	4.26	**0.37**	**0.42**	3.60	-1.64	6.99	2.52
	slope	-1.52	-1.71	-2.80	2.61	-2.33	-2.21	-1.90	**-0.47**	-1.32	-1.94	**-0.23**	-2.53	-1.18
	n	9	9	9	9	9	9	9	9	9	9	9	9	9
July 2002 – July 2023	at least	0.00	16.7	2000	5.17	24,098	3,000	309	1.80	7.82	9.11	0.43	3,740	311
	median	1.92	17.8	2060	5.32	26,720	3,340	433	2.55	11.71	15.90	1.34	4510	448
period	max.	2.86	29.4	2330	5.56	39,480	4,260	607	3.54	14.60	24.30	3.60	5990	499
II.	average	1.79	19.4	2091	5.34	28,416	3,523	458	2.61	11.20	16.12	1.68	4439	423
	standard deviation	0.88	3.5	99	0.10	4070	441	88	0.49	2.07	4.92	1.03	641	65
	rel. var.	1.49	0.71	0.16	0.07	0.58	0.38	0.69	0.68	0.58	0.96	2.36	0.50	0.42
	sharpness	-0.79	3.64	2.70	**0.17**	2.89	-1.01	-0.72	**-0.27**	-0.65	-1.09	-1.13	0.76	-0.67
	slope	**-0.49**	1.90	1.84	**0.37**	1.63	0.65	**0.38**	0.51	**-0.34**	**0.09**	**0.40**	0.86	-1.00
	n	15	15	15	15	15	15	15	15	15	15	15	15	15
August 2023 – Dec. 2024	at least	2.15	31.1	2100	5.12	24,733	1,360	190	0.03	14.70	2.78	0.11	5410	356
	median	4.26	35.5	2370	5.21	26,900	1,990	231	0.69	18.82	5.19	0.43	6100	474
period	max.	5.87	37.6	2490	5.52	30,276	2,570	298	1.10	22.49	6.47	0.81	7110	522
III.	average	3.98	35.1	2304	5.26	27244	2,029	232	0.67	18.70	5.08	0.42	6151	463
	standard deviation	1.10	1.8	131	0.12	1867	293	30	0.22	1.78	0.85	0.17	500	40
	rel. var.	0.87	0.18	0.16	0.08	0.21	0.61	0.47	1.57	0.41	0.71	1.61	0.28	0.35
	peakedness	-0.97	**0.07**	-1.32	**0.10**	-1.42	0.55	**0.05**	4.68	1.07	3.21	0.61	**-0.28**	2.68
	slope	**-0.21**	-0.77	**-0.31**	0.86	**0.22**	**-0.19**	0.75	-1.20	**-0.21**	-1.48	**0.35**	**0.38**	-1.49
	n	17	17	17	17	17	17	17	17	17	17	17	17	17

Explanations: Relative variability = (maximum – minimum)/median; n – number of data points in the data set. The values of kurtosis and skewness indicating the normal nature of the distribution are highlighted in bold.
Explanations: Relative variability = (maximum – minimum)/median; n – number of data points in the dataset. The values of kurtosis and skewness indicating a normal distribution are highlighted in bold.

Mineral saturation of mine water

The water samples from the Gabriela shaft were only slightly undersaturated or in equilibrium with respect to all three types of siderite deposits, as well as pure siderite. At the same time, it was undersaturated with respect to ankerite (B), ankerite (BS) and calcite (B) (Table 7). The sampled mine waters are undersaturated with respect to potential secondary carbonates – calcite, dolomite and nesquehonite. Some of the samples are approaching equilibrium with rhodochrosite, or have reached it. All the samples evaluated are supersaturated with respect to goethite. They are mostly supersaturated with respect to ferrihydrite, or are in equilibrium with it. They are significantly undersaturated with respect to manganite.

Most samples from the spillway at the Gabriela shaft are in equilibrium with gypsum, and some of them are (Table 8). They are undersaturated with respect to other sulphate minerals that may occur in this environment (Table 8). The samples are significantly oversaturated with respect to K-jarozite and more moderately oversaturated, or in equilibrium, with Na-jarozite. The degree of saturation with respect to H-jarozite and Na-jarozite is highly variable and fluctuates around the equilibrium state. The water from the Gabriela shaft is characterised by a high degree of saturation with respect to gaseous CO_2, whilst in some samples it approaches equilibrium. The determined average value of SI_{CO_2}= -0.20 corresponds to a partial pressure $_{of\ CO_2}$of 0.63 atm, and its determined range of variation is 0.29–0.98 atm.

The sampled mine waters are undersaturated with respect to mineral phases concentrating arsenic, nickel and cobalt, the presence of which can be expected in this environment (Table 9).

The data presented suggest that the dissolution of siderite and the precipitation of gypsum from the mine water are among the dominant processes shaping the macrochemical composition of the water flowing out through the Gabriela shaft from the Manó–Gabriela mine. The stable supersaturation of the water with respect to ferrihydrite indicates the possibility of Fe-oxide formation. The precipitation of rhodochrosite likely occurs only occasionally. In terms of the temporal evolution of the saturation state, a relatively significant decrease in the water saturation index with respect to melanterite, rhodochrosite, as well as siderite and calcite, can be observed in the period following a sudden change in water temperature (Fig. 10). The degree of saturation with respect to gypsum, epsomite and carbon dioxide remains stable over time.

Table 6 Spearman's correlations between the basic physicochemical parameters of the water and the concentrations of the main ions dissolved in the water of the Gabriela shaft for the period June 2022 – December 2024.
Table 6 Spearman correlations of basic ions content in the water of the Gabriela shaft adit for the period June 2022 – December 2024.

	t	Q	EC	pH	SO_4^{2-}	Fe	Mn	As	Ni	Co	Mg	Zn	Ca	Tvo
t	1.00	**0.70**	**0.40**	-0.07	**-0.40**	**-0.94**	**-0.97**	**0.71**	**-0.86**	**-0.63**	**0.52**	**-0.85**	**0.42**	**0.64**
Q	**0.70**	1.00	**0.58**	-0.20	-0.28	**-0.66**	**-0.72**	**0.72**	**-0.69**	**-0.46**	**0.61**	**-0.66**	0.27	**0.79**
EC	**0.40**	**0.58**	1.00	**-0.48**	0.25	**-0.47**	**-0.45**	**0.71**	**-0.56**	**-0.59**	**0.80**	**-0.58**	0.20	**0.82**
pH	-0.07	-0.20	**-0.48**	1.00	-0.05	0.11	0.12	-0.31	0.23	**0.41**	**-0.37**	0.13	-0.32	**-0.38**
SO4	**-0.40**	-0.28	0.25	-0.05	1.00	**0.36**	**0.43**	-0.01	0.28	0.12	0.29	0.19	0.00	-0.01
Fe	**-0.94**	**-0.66**	**-0.47**	0.11	**0.36**	1.00	**0.95**	**-0.69**	**0.86**	**0.64**	**-0.50**	**0.82**	**-0.39**	**-0.66**
Mn	**-0.97**	**-0.72**	**-0.45**	0.12	**0.43**	**0.95**	1.00	**-0.67**	**0.90**	**0.64**	**-0.48**	**0.87**	**-0.36**	**-0.69**
As	**0.71**	**0.72**	**0.71**	-0.31	-0.01	**-0.69**	**-0.67**	1.00	**-0.79**	**-0.72**	**0.86**	**-0.77**	0.30	**0.82**
Ni	**-0.86**	**-0.69**	**-0.56**	0.23	0.28	**0.86**	**0.90**	**-0.79**	1.00	**0.80**	**-0.63**	**0.89**	-0.24	**-0.76**
Co	**-0.63**	**-0.46**	**-0.59**	**0.41**	0.12	**0.64**	**0.64**	**-0.72**	**0.80**	1.00	**-0.62**	**0.62**	**-0.37**	**-0.61**
Mg	**0.52**	**0.61**	**0.80**	**-0.37**	0.29	**-0.50**	**-0.48**	**0.86**	**-0.63**	**-0.62**	1.00	**-0.66**	0.28	**0.85**
Zn	**-0.85**	**-0.66**	**-0.58**	0.13	0.19	**0.82**	**0.87**	**-0.77**	**0.89**	**0.62**	**-0.66**	1.00	-0.12	**-0.81**
Ca	**0.42**	0.27	0.20	-0.32	0.00	**-0.39**	**-0.36**	0.30	-0.24	**-0.37**	0.28	-0.12	1.00	0.11
Total	**0.64**	**0.79**	**0.82**	**-0.38**	-0.01	**-0.66**	**-0.69**	**0.82**	**-0.76**	**-0.61**	**0.85**	**-0.81**	0.11	1.00

Explanatory notes: *Q* – discharge rate at the time of sampling, *t* – time elapsed since the mine was flooded. Marked correlations are significant at the level of $p < 0.05$.
Explanations: *Q* – volume of mine water discharge at the time of sampling, *t* – time elapsed since the mine was flooded. Correlations marked with an asterisk are significant at the $p < 0.05$ level.

Table 7 Saturation indices SI of water from the Gabriela shaft with respect to selected carbonate, (oxi)hydroxide and CO_2.
Table 7 Saturation indices *(SI)* of water from the Gabriela shaft with respect to selected carbonate, (oxi)hydroxide mineral phases and CO_2.

Object / pH / Sample			SI-siderite(B) $Fe_{0.892}Mg_{0.058}Ca_{0.006}Mn_{0.052}CO_3$	SI-siderite(V) $Fe_{0.869}Mg_{0.08}Ca_{0.04}Mn_{0.011}CO_3$	SI-siderite(BS) $Fe_{0.774}Mg_{0.068}Ca_{0.006}Mn_{0.152}CO_3$	SI-ankerite(B) $Ca_{1.00}(Fe_{0.676}Mg_{0.26}Mn_{0.064}(CO_3)_2$	SI-ankerite (BS) $Ca_{1.00}(Fe_{0.544}Mg_{0.216}Mn_{0.24}(CO_3)_2$	SI-calcite(B) $Ca_{0.892}Mg_{0.076}Mn_{0.016}CO_3$	SI-calcite $CaCO_3$	SI-dolomite $CaMg(_{CO_3})_2$	SI-siderite $FeCO_3$	SI-nesquehonite $MgCO_3:3H_2O$	SI-rhodochrosite $MnCO_3$	Ferrihydrite $Fe(OH)_3$	SI-goethite FeOOH	SI-manganite MnOOH
			primary carbonate minerals of the deposit						**Hypothetical secondary carbonate minerals**							
Min.	5.12	3.58	-0.91	-0.99	-0.99	-3.89	-3.91	-2.55	-2.69	-3.56	-0.73	-4.02	-1.30	**0.09**	2.84	-10.29
Average	5.32	3.87	-0.46	-0.55	-0.54	-3.05	-3.05	-2.08	-2.24	-2.94	-0.32	-3.75	-0.87	0.89	3.58	-9.31
Max.	5.78	5.33	**0.12**	**0.02**	**0.04**	-2.04	-2.05	-1.65	-1.88	-2.16	**0.15**	-3.12	**-0.29**	2.31	5.08	-7.05

Explanatory notes: siderite(B), ankerite(B), calcite(B) – "basic type" of carbonate mineral in stratiform deposits – so-called metasomatic carbonates; siderite (BS), ankerite (BS) – carbonate minerals in black phyllites, siderite (V) – vein siderite, Manó – Gabriela deposit (Turan, Turanová, 1993). Values indicating the solution equilibrium with respect to the relevant mineral are highlighted in bold.
Explanations: siderite(B), ankerite(B), calcite(B) – "basic type" of carbonate mineral in stratiform beds – so-called metasomatic carbonates; siderite(BS), ankerite(BS) – carbonate minerals in black phyllites, siderite(V) – vein siderite, Manó – Gabriela deposit (Turan, Turanová, 1993). Boldfaced values indicate the equilibrium of the solution with respect to the respective mineral.

Table 8 Saturation indices of water from the Manó – Gabriela mine with respect to selected sulphates and CO_2
Table 8 Saturation indices *(SI)* of mine water with respect to selected sulphate mineral phases and CO_2.

Object / sample	Gypsum $CaSO_4:2H_2O$	Epsomite $MgSO_4:7H_2O$	Melanterite $FeSO_4:7H_2O$	$Fe_2(SO_4)_3$	Celestine $SrSO_4$	$MnSO_4$	Alunite $KAl_3(SO_4)_2(OH)_6$	$AlOHSO_4$	Anglesite $PbSO_4$	K-jarosite $KFe_3(SO_4)_2(OH)_6$	H-jarozite $(H_3O)Fe_3(SO_4)_2(OH)_6$	Na-jarozite $NaFe_3(SO_4)_2(OH)_6$	$SI\text{-}CO_2(g)$
	Sulphates												
Min.	**-0.09**	-1.58	-2.59	-25.77	-1.40	-8.13	0.88	-2.15	-3.84	3.60	-1.70	-0.24	-0.54
Average	**0.12**	-1.03	-2.18	-24.22	-1.16	-7.70	6.10	-0.19	-2.74	5.31	**0.18**	1.50	-0.20
Max.	0.25	-0.83	-1.86	-22.84	-1.01	-7.21	8.10	0.52	-1.85	8.73	2.82	4.86	-0.01

Table 9 Saturation indices of water from the Manó–Gabriela mine with respect to selected mineral phases concentrating arsenic, nickel and cobalt.
Table 9 Saturation indices **(***SI)* of mine water samples with respect to selected As, Ni, and Co-containing mineral phases.

Object / sample	Skorodite $FeAsO_4:2H_2O$	$Mn_3(AsO_4)_2:8H_2O$	As_2O_5	Weilit $CaHAsO_4$	$Ca_3(AsO_4)_2:4H_2O$	$AlAsO_4:2H_2O$	$Ni_3(AsO_4)_2:8H_2O$	Morenosite $NiSO_4:7H_2O$	Retgersite $NiSO_4:6H_2O$	$Ni_4(OH)_6SO_4$	$NiCO_3$	$Ni(OH)_2$	$CoSO_4:6H_2O$	$Co(OH)_2$	$CoSO_4$
Min.	-4.16	-7.46	-23.71	-5.10	-15.07	-5.31	-14.54	-4.79	-4.85	-23.81	-6.25	-7.58	-6.31	-10.00	-11.15
Average	-3.72	-6.47	-21.19	-4.29	-14.01	-3.43	-12.93	-4.21	-4.30	-21.01	-5.65	-6.88	-5.41	-8.91	-10.55
Max.	-2.96	-5.35	-20.21	-3.98	-20.21	-2.84	-11.48	-3.73	-3.83	-16.96	-5.05	-6.05	-4.70	-7.37	-9.97

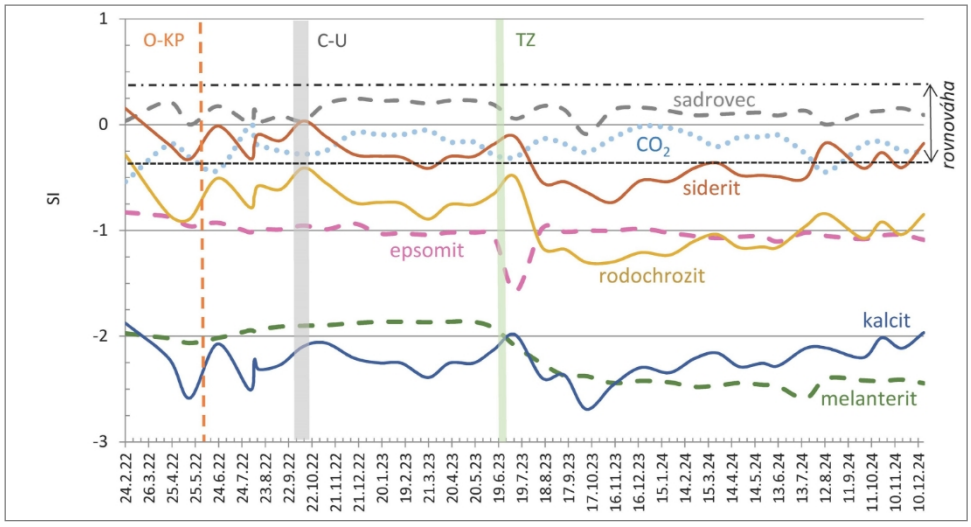

Fig. 10 Time variation of saturation of water outflowing from the Gabriela shaft in respect to selected minerals. Explanations as for Fig. 3.
Fig. 10 Time variation of saturation of water outflowing from the Gabriela shaft in respect to selected minerals. Explanations as for Fig. 3.

Specification modelling of the occurrence of sulphur, iron, manganese, arsenic, nickel and cobalt

According to the results of speciation modelling, sulphur in the mine water of the Gabriela pit occurs not only in the form of the SO_4^{2-}anion (Table 10), but also to a significant extent as the $MgSO_4^{-}$complex (27%–60% of the total amount of S^{VI}), as well as in the form of $CaSO_4^{-}$complexes (2%–5%) and $FeSO_4^{-}$ complexes (2%–8%). Iron in these samples occurs almost exclusively in the second oxidation state (Fe^{II}), with the simple Fe^{2+}ion (70%–81%) dominating over the neutral $FeSO_4$complex. Manganese

in these samples occurs exclusively in the second oxidation state (Mn^{II}), with the simple ion Mn^{2+} dominating (76%–85%) over the neutral complex $MnSO_4$.

The results of the speciation calculation of arsenic forms in the mine water of the Manó–Gabriela mine indicate that it is almost exclusively in oxidation state 5, with H_2AsO^- dominating over $HAsO_4^{2-}$, whilst the proportion of the neutral of the H_3AsO_4 complex is negligible and the AsO_4^{-3} anion is not represented (Table 11). Nickel is present in the water of the Gabriela shaft mainly in the form of the neutral complex $NiSO_4$ (49%–69%), to a lesser extent as the Ni^{2+} ion (22%–44%), and as $NiHCO^+$ complexes (3%–6%) and $Ni(SO_4)^{2-}$ (0.3%–4.5%) (Table 10). Cobalt is present as the cation Co^{2+} (72% – 83%) and, to a significant extent, as the neutral complex $CoSO_4$ (16% – 26%), and only to a lesser extent as the complex $CoHCO^+$.

Table 10 Proportion of sulphur, iron and manganese species in their total mass in water samples from the Manó – Gabriela mine.
Table 10 Sulphur, iron and manganese species in mine water samples from the Manó – Gabriela mine.

	SO_4^{-2} – % of S(6)	$MgSO_4$ – % of S(6)	$CaSO_4$ – % of S(6)	$FeSO_4$ – % of S(6)	% Fe-II of total Fe	Fe^{+2} of Fe(2)	$FeSO_4$ of Fe(2)	$FeHCO_3^+$ of Fe(2)	Mn^{+2} of Mn(2)	$MnSO_4$ from Mn(2)
Min.	33.7	26.9	1.6	2.0	99.78	69.5	19.4	0.05	75.8	14.9
Average	42.5	49.7	2.7	4.3	99.99	76.1	23.8	0.10	81.4	18.5
Max.	58.7	59.9	5.3	7.9	100.00	80.6	30.3	0.23	85.0	23.8

Table 11 Proportion of arsenic As^V, nickel Ni^{II} and cobalt Co^{II} species in their total mass in selected water samples from the Manó – Gabriela mine.
Table 11 Arsenic As^V, nickel Ni^{II} and cobalt Co^{II} species in mine water samples from the Manó – Gabriela mine.

	% As-V from As-total	$HAsO_4^{2-}$	$H_2AsO_4^-$	$H3AsO4$	Ni^{+2}	$NiSO4$	$Ni(SO_4)^{2-}$	$NiHCO_3^+$	Co^{2+}	$CoSO_4$	$CoHCO_3^+$
Min.	99.18	14.4	54.6	0.01	22.4	49.3	0.3	3.4	71.9	16.1	0.6
Average	99.87	22.9	77.1	0.03	30.1	62.5	2.2	5.1	79.0	19.9	1.0
Max.	100.00	45.3	85.6	0.05	44.4	69.0	4.5	6.4	83.1	26.1	2.0

DISCUSSION

When considering the formation of the chemical composition of the mine water flowing from the Gabriela shaft, it is necessary to take into account the hydrogeological conditions of the mine. The mine workings at the Manó–Gabriela deposit are excavated in a rock environment of Palaeozoic crystalline limestones and ore carbonates (siderite, ankerite) surrounded by metamorphic rocks (mainly phyllites) of the Gemer region. Since karst phenomena have not developed in either the crystalline limestones or the ore carbonates, the fracture-type permeability dominates in them. The rock environment of this mine therefore has the character of a hydrogeological massif (in the sense of Jetel, in Hanzel 1990), which is characterised by groundwater circulation concentrated mainly in the near-surface weathering zone and, at greater depths, only locally in fracture zones. Inflows into the mines, excavated within the hydrogeological massif, therefore mostly originate primarily from the near-surface zone of the massif, reached by mining works, or by infiltration of precipitation or surface water through caving reaching the surface or through zones of gravitational fractures in their overburden. However, the relatively low variability in the discharge rate from the Gabriela shaft (2.15 $l \cdot s^{-1}$ – 5.87 $l \cdot s^{-1}$ in the period July 2023 – XII. 2024) suggests, however, that the proportion of direct seepage of surface water into the mine out of the total volume of mine water is very small, if not negligible. The volume of inflows from deeper parts of the massif below the near-surface zone is small, as evidenced by records of the volume of water pumped from the horizons during the mining period. Water infiltrating the mine descends by gravity through its aerated zone (unsaturated zone) to the water level in its saturated zone, becoming enriched by the dissolution of minerals. No reliable data are available on the chemical composition of these seepages. In the final report containing the calculation of the deposit's reserves (Mihók, Jančura, 2000), for example, it is merely stated that the mine waters are generally low in mineral content. According to data on the chemical composition of shallow groundwater obtained during regional hydrogeological research, the mine is primarily infiltrated by surface water from the near-surface zone of the Palaeozoic metamorphic massif, with a total water mineralisation of up to 0.5 $g \cdot l^{-1}$, a slightly alkaline reaction, of the $Mg\text{-}Ca\text{-}HCO_3$ chemical type and a low concentration of metals and metalloids, ranging in the order of $\mu g \cdot l^{-1}$, up to a maximum of the first few tens of $\mu g \cdot l^{-1}$ (Scherer et al., 1999). Based on these findings, it is clear that a significant increase in water mineralisation within the mine's hydrogeological system occurs only within the area of its mining operations in the deposit. A representative of a hydrogeologically and geochemically similar environment in the aeration zone is the Železník siderite mine, from which slightly acidic mine water with a pH of 6.0–6.3 and a total mineralisation of 2.5 $g \cdot l^{-1}$ – 4.7 $g \cdot l^{-1}$, a sulphur concentration of 1.7 $g \cdot l^{-1}$ – 3.3 $g \cdot l^{-1}$, Fe 0.07 $g \cdot l^{-1}$ – 0.16 $g \cdot l^{-1}$ and Mn 0.13 $g \cdot l^{-1}$ – 0.25 $g \cdot l^{-1}$, of the $Mg\text{-}Ca\text{-}SO_4$ chemical type (Bajtoš, 2012). Locally – in the environment of black shales with a high concentration of pyrite and arsenopyrite – there is

In the aeration zone of the Manó–Gabriela mine, water of a similar chemical composition to that found in the Smolník mine could have formed, with a stratiform pyrite deposit in Palaeozoic metamorphic rocks: with a pH of 2.0–4.0, a concentration of dissolved substances of 1.5 $g \cdot l^{-1}$ – 13.8 $g \cdot l^{-1}$, SO_4 1.0 $g \cdot l^{-1}$ – 8.8 $g \cdot l^{-1}$, Fe 5 $mg \cdot l^{-1}$ – 105 $mg \cdot l^{-1}$, Mn 13 $mg \cdot l^{-1}$ – 90 $mg \cdot l^{-1}$ (Finta, Rozdobuďková, 1987). This is the result of intensive oxidation of sulphides in an environment of silicate rocks devoid of carbonate minerals. The Manó–Gabriela mine therefore represents a spatially highly geochemically variable environment, suggesting a considerably variable chemical composition of the water in the gravitationally descending seepage. The nature of the ongoing geochemical processes differs significantly between the unsaturated and saturated (flooded) parts of the mine – the unsaturated zone (aeration zone) and the saturated zone.

The rapid increase in the mineralisation of mine water following the emergence of a seepage after the mine was flooded, compared to the mineralisation of water pumped during the mining period, can be described as a typical phenomenon. In the literature, this is referred to as "first flush". It has also been documented in other ore deep mines in the Slovak Ore Mountains, as well as abroad (e.g. Bajtoš, 2009; 2024; Grmela, 1998; Wolkersdorfer, 2008). Increased mineralisation of the outflowing water from a flooded mine generally decreases gradually, with the period required for the chemical composition of the water to stabilise lasting several years or several decades, sometimes even a century (Younger, 1997; Demchak et al., 2004). This can be explained by the gradual decrease in the proportion of water that originally stagnated in the mine workings for a long time (during the flooding of the mine) – highly mineralised water – relative to the total volume of water flowing out of the mine after its flooding. The increased mineralisation of stagnant mine water is a consequence of the dissolution of easily soluble mineral phases, which formed during the mining period under aerobic conditions, up to a high state of saturation with these minerals. Another factor contributing to the decrease in water mineralisation at the mine outlet is the gradual depletion of these easily soluble mineral phases – a reduction in the total reaction surface area. The concentration of Fe, Mn, Al and As in mine water is also influenced by any change in pH – E_H conditions, particularly a decrease in E_H in the stagnant mine water zone and a subsequent increase *in* E_H in the flow zone created after the mine was flooded.

Dominant hydrochemical processes shaping the macrochemical composition of mine water under standard conditions in the unsaturated zone of the Manó–Gabriela mine

The hydrogeochemical conditions of the Manó–Gabriela mine and the documented chemical composition of its mine water indicate that the main geochemical process occurring in its aeration zone is the dissolution of Fe-carbonates from the deposit in combination with the oxidation of sulphides, particularly pyrite and arsenopyrite. Pyrite is dispersed both in the Fe-carbonates themselves, but also in the associated phyllites. The intensity of carbonate dissolution is significantly influenced by protons released during the oxidation of sulphides.

In the unsaturated part of the mine – in the aeration zone – the ongoing oxidation of pyrite by O_2 dissolved in water and the subsequent precipitation of ferrihydrite produces 4 protons (reaction 1), whilst the similar oxidation of arsenopyrite (reaction 2) produces 3 protons per 1 mol of sulphide. The rate of arsenopyrite oxidation by oxygen is slightly lower than that of pyrite (Mok, Wai, 1994). Under conditions of high evaporation, the product of pyrite oxidation may be melanterite (equation 4). The process of sulphide oxidation can be significantly accelerated by microbial activity, involving the breakdown of the sulphide molecule and the subsequent oxidation of Fe^{2+} to Fe^{3+} (equation 6). As this process is dependent on the presence of oxygen, it is restricted to aerobic environments (Nordstrom, Southam, 1997; Nordstrom, Alpers, 1999). The oxidation of pyrite by the ferric ion Fe^{3+} (Equation 3) begins to predominate over oxidation by oxygen in an acidic environment, at pH < 4 (Singer, Stumm, 1970; Equation 3), when Fe^{3+} is stable in solution.

$$FeS_2 + 3.75\ O_2 + 3.5\ H_2O \rightarrow Fe(OH)_3 + 2\ SO_4 + 4\ H \quad (1)$$

$$FeAsS + 3.5\ O_2 + 6\ H_2O \rightarrow Fe(OH)_3 + SO_4^{2-} + HAsO_4^{-} + 3\ H^+ \quad (2)$$

$$FeS_2 + 14\ Fe^{3+} + 8\ H_2O \rightarrow 15\ Fe^{2+} + 2\ SO_4^{2-} + 16\ H^+ \quad (3)$$

$$FeS_2 + 8H_2O + 7O_2 \rightarrow FeSO_4 * 7H_2O + SO_4^{2-} + 2H^+ \quad (4)$$

Protons released into the solution by the oxidation of sulphide minerals by oxygen (reactions 1–2), or possibly by Fe^{3+} cations (equation 3) can be neutralised by the dissolution of Fe-carbonates in the deposit, e.g. siderite-B (equation 5; similar equations apply to siderite-V and siderite-BS), ankerite-B (equation 6) and calcite-B (equation 7). During the dissolution of ankerite and siderite, Mg, Ca, Fe and HCO^- are thus released into the solution, along with small amounts of Mn. The released Fe^{2+} ions in the unsaturated zone of the mine oxidise to Fe^{3+} (Equation 8), which, at a solution pH higher than 4, precipitate (Equation 9) from the solution upon the release of protons (Moses et al., 1987; Ehrlich, 1996; Nordstrom et al., 1997).

$$Fe_{0.892}Mg_{0.050}Ca_{0.006}Mn_{0.052}CO_3 + H^+ \rightarrow 0.892\ Fe^{+2} + 0.050\ Mg^{+2} + 0.006\ Ca^{2+} + 0.052\ Mn^{2+} + HCO_3^- \quad (5)$$

$$Ca_{1.00}(Fe_{0.676}Mg_{0.26}Mn_{0.064}(CO_3)_2 + 2\ H^+ \rightarrow Ca^{+2} + 0.676\ Fe^{+2} + 0.260\ Mg^{+2} + 0.064\ Mn^{+2} + 2\ HCO_3^{-2} \quad (6)$$

$$Ca_{0.892}Mg_{0.076}Mn_{0.016}CO_3 + H^+ \rightarrow 0.892\ Ca^{+2} + 0.076\ Mg^{+2} + 0.016\ Mn^{2+} + HCO_3^{-2} \quad (7)$$

$$Fe^{2+} + 0.25\ O_2 + H^+ \rightarrow Fe^{3+} + 0.5\ H_2O \quad (8)$$

$$Fe^{3+} + 3H_2O = Fe(OH)_3 + 3H^+ \quad (9)$$

In the unsaturated part of the mine, therefore, there is a permanent precipitation of ferric oxide (ferrihydrite – goethite). During mining operations, when the mine was dewatered by pumping, this affected the entire mine area, from the surface to the deepest levels.

The intensity of pyrite oxidation is influenced by its mineralogical characteristics and external chemical, physical and biological factors. Mineralogical characteristics include particle size, porosity, surface area, crystallography and concentration of trace elements. External factors include the presence of other sulphides, the presence of microorganisms, the concentration of oxygen and carbon dioxide, temperature, pH

and the Fe^{2+}/Fe^{3+} ratio of the reacting solution (Lottermoser, 2010). An indirect indicator of the intensity of oxidation
The concentration of sulphates in mine water is due to the presence of pyrite in the mine's aeration zone in the absence of significant quantities of sulphate minerals. Such data are not available from the Manó–Gabriela mine. Based on an analogy with the siderite mine in Sirk and the pyrite mine in Smolník (much higher pyrite concentration and absence of carbonates with a strong neutralising effect), it can be expected that the sulphate concentration in the mine water of the unsaturated zone of the Manó – Gabriela under standard atmospheric conditions should range from a few $g \cdot l^{-1}$ to a maximum of 5 $g \cdot l^{-1}$.

The influence of spontaneous heating of the black phyllite fillings on the macrochemical composition of mine water

In addition to the presence of atmospheric oxygen, the geochemical processes occurring in the mine's aeration zone were significantly influenced locally by the self-heating of fillings in black phyllites with high concentrations of pyrite and graphite. Hot pillars formed here, similarly to coal deposits, as a result of the oxidation and self-heating of pyrite. At the Manó–Gabriela mine, such hot pillars occurred in the central part of the Manó deposit on the IX and X horizons from 1985, when they were indicated by high concentrations of SO_2 in the mine air (Mihók, 1997b). Despite the miner's efforts, it was not possible to completely eliminate them even by the end of mining operations.

The spontaneous heating of pyrite proceeds in three phases (Rosenblum et al., 2001). The first phase occurs at temperatures up to 100 °C and is expressed in simplified form by exothermic reaction 1. The second phase is characterised by a temperature range of 100 °C – 350 °C, during which the oxidation of pyrite continues with the formation of FeOOH, the thermal decomposition of pyrite begins with the formation of pyrotite $Fe_{(1-x)}S$ (where x = 0 – 0.17), and subsequently elemental sulphur is also produced. In the presence of oxygen, this sulphur oxidises to gaseous SO_2 and, in addition to water vapour, CO_2 is also released from the rock containing organic carbon. If siderite is present, it oxidises to FeO and CO_2 . In addition to the oxidation of pyrite, the sources of heat in this phase are , carbon oxidation, the oxidation of CO to CO_2 and the oxidation of S to SO_2 (Rimstidt, Vaughan, 2003; Lowson, 1982). In the third phase, at temperatures above 350 °C, more intense oxidation of pyrite occurs, forming $Fe_2O_3$and producing SO_2, whilst the oxidation of organic carbon yields CO_2. In this phase, spontaneous combustion of pyrite or organic carbon may occur. The most intense decomposition of pyrite occurs at 400 °C, and up to 900 °C it proceeds according to the following reactions (Li et al., 2019):

$$FeS_2 \rightarrow FeS_x + (1 - x/2)S_2 \quad (10)$$

$$S_2 + 2O_2 \rightarrow 2SO_2 \quad (11)$$

$$2SO_2 + O_2 = 2SO_3 \quad (12)$$

$$FeS_x + (1.5 + 2x)O_2 \rightarrow Fe_2O_3 + 2xSO_2 \quad (13)$$

$$2FeS_x + (3 + 2x)O_2 \rightarrow Fe_2(SO_4)_3 + (2x - 3)SO_2 \quad (14)$$

$$FeS_x + (1 + x)O_2 \rightarrow FeSO_4 + (x - 1)SO_2 \quad (15)$$

In addition to iron sulphates (equations 12 and 13), the formation of other sulphates, such as $CaSO_4$ or $MgSO_4$, can also be expected during the thermal decomposition of ore carbonates. The thermal decomposition of siderite occurs at temperatures of 350 °C – 550 °C; the decomposition temperature of ankerite is influenced by the ratio of Ca, Mg and Fe in the crystal lattice and ranges from 500 to 700 °C. The thermal decomposition of calcite occurs at temperatures of 825 °C – 900 °C, and even higher in a CO_2 atmosphere. The gaseous product of the thermal decomposition of carbonates is CO_2. In a humid environment, the gases released during combustion could, after condensation, increase the acidity of the solutions, which could increase the dissolution rate of the present carbonates (Equations 3–5) and silicate minerals, compared to standard atmospheric conditions. Of the silicate minerals, the main varieties present in black phyllites are sericite (Equation 14) and chlorite (Equation 15). During the subsequent evaporation of the solutions formed by the action of acidic condensates on ore carbonates, muscovite or chlorite, melanterite, epsomite, gypsum, rhodochrosite, jarosite and possibly other sulphate minerals may have precipitated.

$$KAl_3Si_3O_{10}(OH)_2 + 10H^+ = K^+ + 3Al^{+3} + 3H_4SiO_4 \quad (14)$$

$$Mg_5Al_2Si_3O_{10}(OH)_8 + 16H^+ = 5Mg^{+2} + 2Al^{+3} + 3H_4SiO_4 + 6H_2O \quad (15)$$

In addition to the processes mentioned above, increased microbial activity, caused by a rise in temperature – to its optimum range – in suitable zones around the combustion foci, may also have contributed to the increased mineralisation of the mine water. The intensity of oxidation increases almost twofold for every 10 °C rise in temperature (Smith et al. 1992 in Lottermoser, 2010), whilst the temperature optima for the reproduction of mesophilic microorganisms (e.g.

Acidithiobacillus ferrooxidans, *Leptospirillum ferrooxidans*) is approximately 25 °C – 35 °C, for moderately thermophilic species (e.g. *Acidithiobacillus caldus*, *Leptospirillum ferriphilum*) 40 °C – 50 °C, and for thermophilic to extremely thermophilic species (e.g. *Sulfolobus metallicus*, *Metallosphaera sedula*) 65 °C – 80 °C.

Dominant hydrochemical processes shaping the macrochemical composition of mine water in the saturated zone of the Manó–Gabriela mine

During the mine flooding period, whilst the water level rose gradually from August 2011 to February 2022, the volume of flooded mine spaces increased, and with it the reaction surface area of easily soluble sulphates and other secondary minerals formed during the mine's operational period. As a result of their dissolution, as well as the dissolution of the deposit's carbonates by acidic mine water until carbonate equilibrium was reached, the mineralisation of the accumulated mine water increased, mainly through a rise in the concentration of sulphates, iron, magnesium and calcium. The oxidation of sulphides did not occur to any significant extent under such anaerobic conditions. Given the presence of local heating of the rock mass, as a result of long-term pyrite combustion, these were likely not static conditions, but rather circulation of mine water driven by a thermolift. The concentration of calcium dissolved in the water of the Manó–Gabriela mine is likely controlled by gypsum precipitation (Table 7). Magnesium reaches significantly higher concentrations than calcite, suggesting that it does not precipitate in significant quantities – the mine water, upon emerging to the surface, remains significantly undersaturated with respect to dolomite and nesquehonite (Table 7). The relatively high concentration of potassium in the mine water, as a product of sericite dissolution, indicates the importance of the black phyllite environment in shaping its chemical composition.

The documented concentration of sulphates dissolved in the mine water of the Gabriela shaft is significantly higher (5 to 8 times) than the maximum level (see above) that can be expected for the conditions of the unsaturated zone of this mine. Given the practically negligible rate of pyrite oxidation in the saturation zone, the source of the high concentration of SO^{2-} in the water can be attributed to sulphate minerals present in the flooded mine workings and excavations. The spontaneous heating and combustion of pyrite, which occurred during mining and the flooding of the mine, led to an intensification of the precipitation of secondary sulphates and the oxidation of pyrite. Mine water from the unsaturated zone, which filled the mine during its flooding, therefore already exhibited higher mineralisation compared to standard atmospheric conditions. This difference was further accentuated after the mine was flooded, concentrating a larger volume and thus also the reaction surface of secondary minerals.

Origin of arsenic and nickel in mine water

The primary main source of arsenic in mine water can be considered to be the oxidation of sulphides under aerobic conditions. Of these, arsenopyrite and pyrite are dominant, with isomorphous arsenic substitution (Equations 1 and 2). During the combustion of arsenopyrite (Equation 16), arsenic vapours and $_{SO_2}$ may have been released into the mine atmosphere. These then hydrolysed in the presence of water to form arsenious acid $_{H_3AsO_3}$, which dissociates into protons $^{H^+}$ and arsenite ions. The combustion products thus represent a secondary source of arsenic, present in dissolved form in mine water. During the wet oxidation of pyrite and arsenopyrite under acidic conditions, further reactions may also occur (17–19), producing acidity and dissolved forms of arsenic (Kim et al., 2024).

$$2\ FeAsS + 5\ _{O_2} \rightarrow\ _{Fe_2}O_3\ +\ _{As_2O_3}\ +\ 2\ _{SO_2} \quad (16)$$

$$FeS_2\ +\ 7\ Fe_2\ (SO_4\ )_3\ +\ 8\ H_2\ O \rightarrow 15\ FeSO_4\ +\ 8\ H_2\ SO_4 \quad (17)$$

$$2\ FeAsS + 13\ Fe_2\ (SO_4\ )_3\ +\ 16\ H_2\ O \rightarrow 28\ Fe_{SO_4}\ +\ 2\ H_{3AsO_4}\ +\ 13\ H_{2SO_4} \quad (18)$$

$$2\ H_{3AsO_4}\ +\ _{Fe^{2+}(SO_4)^{3-}} \rightarrow\ 2\ _{FeAsO_4}\ +\ 3H_{2SO_4} \quad (19)$$

Arsenic released into the solution in the unsaturated zone of the mine may gradually bind to iron-bearing ochre, which forms and accumulates in the mine workings. The high capacity of both amorphous and crystalline Fe^{III} oxyhydroxides to incorporate metalloids into their structure via adsorption or coprecipitation is well known (Pitter, 1999; Dixit, Hering, 2003; Leuz et al., 2006). At higher E_H levels (from +200 to +500 mV), arsenic adsorbs onto ferrihydrite predominantly as As^V, as As^{III} adsorbs more weakly under these conditions (Pierce, Moore, 1982). Furthermore, the Fe^{III}-As^{III} complex is more soluble than the Fe^{III}-As^V complex (Gulens et al., 1973). With a gradual decrease in redox potential (oxygen deficiency), As^V is reduced to As^{III} (Masscheleyn, Patrick, 1994), leading to the release of some of the sorbed As due to the weaker binding of As^{III} to ferrihydrite. When Eh falls below
At +100 mV, ferrihydrite begins to dissolve, releasing bound arsenic through sorption and coprecipitation (Masscheleyn, Patrick, 1994; Deutsch, 1997). This process may have occurred during the flooding of the mine, through the consumption of oxygen dissolved in the mine water of the saturated zone, during the oxidation of sulphides and Fe^{2+}. The documented E_H values in samples of water flowing out of it are mostly in the range of +180 to +240 mV (Fig. 11). The absence of any influence of ferrihydrite dissolution on fluctuations in As concentration in the mine water is also indicated by the graph showing the relationship between As concentration and Fe (Fig. 12 – the expected positive correlation is absent in this case). The rate of As sorption onto ferrihydrite also depends on the pH of the solution – it is assumed that As is released into the solution as the pH increases (Welch et al., 1988; Robertson, 1989; Smedley et al.,

2003). However, the documented pH values fall within a relatively narrow range of 5.02–5.56 – suggesting a negligible effect on changes in As concentration in the mine water of the Gabriela pit.

The primary source of nickel in the mine water is the oxidation of sulphide minerals, the presence of which has been confirmed at the deposit (Grecula et al., 1995): gersdorite (NiAsS), ullmanite (NiSbS), pentlandite ($Fe_{4,5}$ $Ni_{4,5}$ S_8), Millerite (NiS), violarite ($FeNi_2$ S_4). Of these, gersdorfit is the most abundant, which thermally decomposes into gaseous SO_3 , arsenic vapours and solid NiO. In a humid environment at temperatures of 300 °C – 500 °C, nickel sulphate may form through the reaction of NiO with acidic mine water (reaction 21), which is a secondary source of nickel in the mine water. During the combustion of pentlandite and violarite, the formation $_{of\ NiSO_4}$and $_{FeSO_4}$can be similarly assumed. Ullmanite is not a significant source of Ni, as evidenced by the low concentration of Sb in the mine water.

$$NiO + H_2SO_4 \rightarrow NiSO_4 + H_2O \quad (21)$$

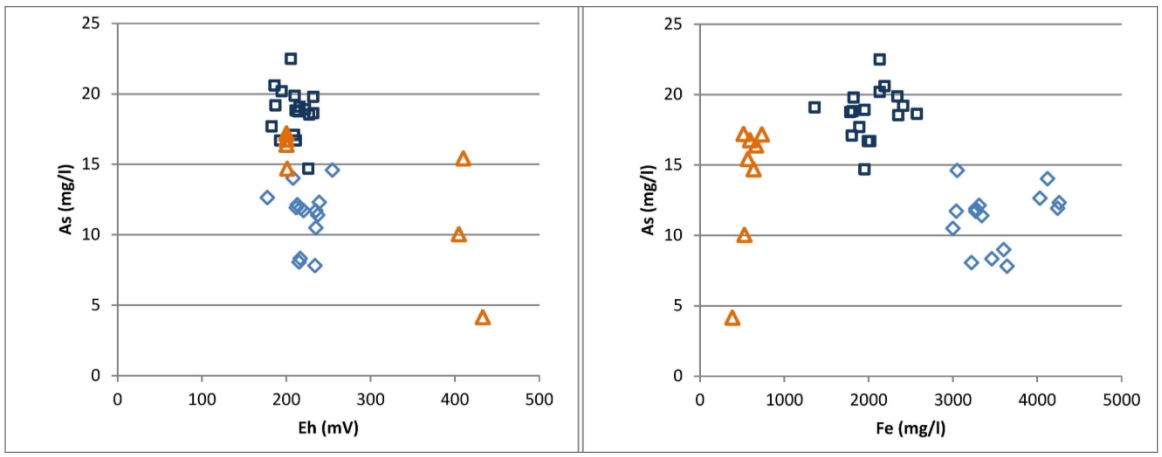

Fig. 11 (left) As concentration and EH values in the mine water of the Gabriela shaft.
Legend: triangles – samples from the period II. 2022 – VI. 2022, squares – samples from the period VI. 2022 – VII. 2023, diamonds – samples from the period VIII. 2023 – XII. 2024.

Fig. 12 (right) Concentrations of As and Fe in mine water from the Gabriela shaft.
Legend: triangles – samples from the period February 2022 – June 2022, squares – samples from the period June 2022 – July 2023, diamonds – samples from the period August 2023 – December 2024.

Conceptual model of the origin of the anomalous chemical composition of water in the Manó – Gabriela mine

Based on the data obtained and their interpretation, the following conceptual model, divided into three developmental periods, can be proposed to explain the origin of the extremely highly mineralised water in the Manó – Gabriela siderite mine:

1) the period of mine operation, when the entire mine area was an unsaturated zone: the dominant geochemical process throughout the mine area is a combination of the dissolution of ankerite, siderite and calcite with the oxidation of pyrite and, locally, arsenopyrite by oxygen (Equations 1–7), leading to the precipitation of iron oxyhydroxides (Equation 9), locally, however, in areas where black phyllites occur, the oxidation of pyrite and arsenopyrite with the formation of acidic mine drainage (AMD) may have dominated (Equations 1–3), whilst spontaneous heating/combustion of their waste heaps beneath the roof collapses of the workings produced sulphate minerals of Fe, Mg and Ca and the gases SO_3 and CO_2 , which, upon condensation, locally increased the acidity of the environment (Equations 8–13) with subsequent intensive dissolution of carbonates and also the heating of the surrounding rock mass to a high temperature, whilst the increased temperature in the vicinity may have intensified the activity of microorganisms in the oxidation of pyrite,
2) the period of mine flooding, when an increasingly larger part of the mine gradually came under the water level into the saturated zone: the dominant geochemical processes in the saturated part of the mine were the dissolution of secondary sulphates (efflorescent salts) and the dissolution of ore carbonates, controlled by the partial pressure $_{of\ CO_2}$and the pH of the solution, under conditions of water circulation generated by a thermolift caused by localised heating of the massif following the burning of rockfalls,
3) the period following the flooding of the mine and the emergence of the outflow through the Gabriela shaft: the processes described above continue in both the saturated and unsaturated parts of the mine, whilst in the saturated zone the quantity of secondary sulphates gradually decreases through their dissolution and the removal of dissolved components, and a regime of mine water circulation forms in the saturated zone under the influence of hydraulic and thermal factors (a

a thermolift generated by localised heating of the rock mass following the burning of rockfalls) and by the varying density of the mine water resulting from significant differences in its mineralisation across different parts of the mine.

More pronounced stratification of mine water in the saturated zone of the mine likely occurred only in parts outside the reach of the thermolift generated by zones of the rock mass that were heated by the burning of rockfalls in black phyllites during the period of aerobic conditions. The documented high temperature of the water flowing out of the mine via the Gabriela shaft significantly exceeds the expected temperature of 10 °C – 15 °C based on the geothermal gradient. It also suggests the continuing influence of spontaneous pyrites heating processes on the circulation and formation of the chemical composition of the water in the Manó–Gabriela mine. Given the spatial extent of the mining operations, the area where they may occur is the space on the underlying blocks of the Manó deposit just above the water table (and within the zone of its seasonal fluctuation), east of the Manó II shaft. All overburden mining operations at the Manó deposit, as well as those at the Gabriela deposit, are located below the water table, where no significant exothermic processes are expected to occur. To better explain the high temperature of the water flowing out of the Gabriela shaft, it is necessary to study the geothermal conditions of the mine using model calculations of heat accumulation in the rock and its exchange with mine water following the flooding of hot waste heaps, supported by vertical profiles of water temperature in the mine and measurements of $_{CO_2}$and $_{SO_2}$concentrations in the mine air.

CONCLUSION

Monitoring of the chemical composition of the mine water flowing out through the Gabriela shaft from the Manó–Gabriela siderite mine – carried out with monthly sampling during the first three years following the flooding of the mine – documented the temporal evolution of the concentrations of environmentally hazardous elements dissolved in the water, as well as its macrochemical composition. Initially, the water—which was low in mineral content and slightly alkaline, and began to flow out of the shaft via an overflow after the mine was flooded—became, within less than 10 days, highly mineralised (up to 40 $g \cdot l^{-1}$), acidic mine water with an extremely high concentration of SO^{2-}_4, Mg, Fe, Mn, As, Ni, and high concentrations of Co, Al and Zn. This change was a manifestation of vertical water stratification, which developed in the Gabriela shaft during its flooding, due to the inflow of low-mineralised shallow groundwater from the Jozef adit. In the following period, two significant changes in water flow occurred in the mine, which manifested themselves as changes in the temperature and chemical composition of the water flowing out of the Gabriela shaft. The first change was related to a technical intervention to stop water inflow, flowing from the area outside the Manó–Gabriela mine via the Kobeliarovský crosscut at a rate of approximately 16 $l \cdot s^{-1}$ into its central section through an unnamed chimney near the Manó II blind shaft, in June 2022. The second change was likely the result of the resumption of part of the water flow from the Kobeliarovský adit, estimated at around 2 $l \cdot s^{-1}$, into the chimney near the Manó II shaft, due to a leak in the dam. In both cases, the most significant change was in water temperature (a drop from 36 °C to 17 °C and a rise from 18 °C to 34 °C, respectively); significant changes also occurred in the concentration of SO^{2-}_4 (a drop from 40 $g \cdot l^{-1}$ to 26 $g \cdot l^{-1}$ and an increase from 24 $g \cdot l^{-1}$ to 30 $g \cdot l^{-1}$, respectively) and Mg (a decrease from 6 $g \cdot l^{-1}$ to 5 $g \cdot l^{-1}$ and an increase from 5 $g \cdot l^{-1}$ to 6 $g \cdot l^{-1}$, respectively). However, the aforementioned changes in water flow in the mine did not have a significant impact on the concentrations of Fe and Mn, which showed a continuous decline with a statistically significant exponential trend throughout the entire monitoring period. A statistically significant downward trend is consistent with the assumption (the first flush phenomenon) documented for part of the monitoring period following the second change in mine flow for total water mineralisation, and the concentrations of SO^{2-}_4, Mg, Al and Zn. Co concentrations and pH values showed a statistically significant upward trend during the aforementioned part of the monitoring period. In contrast, arsenic concentrations are highly variable over time, which is likely a reflection of the high spatial variability of its source minerals within the mine.

An analysis of the hydrogeochemical conditions and mining-technological factors at the Manó – Gabriela, supported by geochemical calculations/modelling using the PREEQC programme, shows that the primary dominant hydrogeochemical process shaping the chemical composition of the mine water is the dissolution of Fe-carbonates from the deposit in combination with the oxidation of sulphides, particularly pyrite and arsenopyrite. The intensity of carbonate dissolution is significantly influenced by protons released during the oxidation of sulphides, as well as by the relatively high partial pressure of CO_2. The nature of these processes differs considerably between the unsaturated and saturated (flooded) parts of the mine. Anomalously high concentrations of SO^{2-}_4, Mg, Fe, As and Ni in mine water may be linked to the presence of black phyllites in the immediate overburden of the siderite deposit. In the environment of waste heaps formed by black phyllites, which were left in the workings, acidic solutions (the AMD or ARD phenomenon) may have formed, which could have intensified the dissolution of ore carbonates beyond the level typical in a siderite mine with ore of an analogous genetic type. Furthermore, spontaneous heating and even self-ignition of pyrite occurred here, exacerbated by the presence of organic carbon in the phyllites. As a result of these thermal processes, beyond the standard atmospheric conditions of the mine: 1) at temperatures up to 80 °C, areas of thermal optimum could form for the growth of microorganisms accelerating the oxidation of pyrite, 2)

the acidity of the environment increased (condensates of thermally released SO_2 and CO_2 gases further increased the rate of carbonate dissolution), 3) the volume of secondary sulphates increased, which raised the mineralisation of the water following the flooding of the mine. However, the extent to which these secondary processes contributed to the level of water mineralisation cannot be quantified more precisely based on the available data. The burning of black phyllites likely also resulted in the release of arsenic vapours, which, upon condensation, contributed to the increased concentration of arsenic in the mine water.

To forecast the future development of the chemical composition of the mine water flowing through the Gabriela shaft into the Marta adit and then to the surface after mixing with water from the Kobeliarovský crosscut, it is important to consider the possible influence of the thermolift on water flow in the flooded (saturated) part of the mine. As a result of the burning of rockfalls, the resulting zones of rock mass heating may have generated an upward current in the central part of the mine and are driving deep circulation, which prevents the development of water stratification with a stable upper layer of less mineralised water, which would be favourable from an environmental perspective. The timeframe of this impact and its persistence to the present day remains unspecified for the time being. However, it is also possible that the influence of spontaneous heating of pyrite on the circulation and formation of the chemical composition of the water in the Manó–Gabriela mine, in the workings just above the water table.

To gain a better understanding of the hydrogeochemical processes occurring in the mine, it is necessary to monitor and continuously evaluate vertical changes in the chemical composition, redox conditions and temperature of the mine water at accessible locations. To better explain the high temperature of the water flowing out of the Gabriela shaft, it is necessary to study the mine's geothermal conditions using model calculations of heat accumulation in the rocks and their exchange with mine water following the flooding of hot waste heaps, supported by vertical profiles of water temperature in the mine and measurements of CO_2 and SO_2 concentrations in the mine air.

In principle, however, it is possible to anticipate a gradual, slow decline in its temperature, mineralisation, and the concentration of environmentally hazardous elements dissolved in it over the coming period.

ACKNOWLEDGEMENTS

The results of this study were obtained thanks to the state monitoring project 'Partial Monitoring System – Geological Factors', coordinated by the Ministry of the Environment of the Slovak Republic.

REFERENCES

BAJANÍK, Š., IVANIČKA, J., MELLO, J., REICHWALDER, P., PRISTAŠ, J., SNOPKO, L., VOZÁR, J., VOZÁROVÁ, A. 1984: *Geological Map of the Slovak Ore Mountains. Eastern Part*. Bratislava, GÚDŠ.

BAJTOŠ, P. 2009: Changes in water quality of selected watercourses in the Slovak Ore Mountains during and after the extraction of ore deposits. In: *Rapantová, N., Grmela, A. (Eds.): Proceedings of the 10th Czech-Slovak International Hydrogeological Congress, Ostrava, 31 August – 3 September 2009*. Ostrava, VŠB – Technical University of Ostrava, pp. 205–208.

BAJTOŠ, P. 2012a: Mass flow balance of contaminants in mountainous areas affected by mining activities, using the example of the Dúbrava Sb deposit and the Slovinky Cu deposit. *Groundwater*, 18, 1, pp. 110–122.

BAJTOŠ, P. 2012b: Hydrogeochemical modelling of weathering at the depleted Železník siderite deposit, Slovak Ore Mountains. *Mineralia Slovaca*, 44, 2, pp. 199–212.

BAJTOŠ, P. 2016: Mine Waters in the Slovak Part of the Western Carpathians – Distribution, Classification and Related Environmental Issues. *Slovak Geological Magazine*, 16, 1, pp. 139–158.

BAJTOŠ, P. 2022: Use of analysis of seasonal hydrochemical regime for better understanding of mine water genesis and more accurate estimate of its impact on stream water quality at the flooded Rudňany ore mine (North-Gemeric zone, Slovakia). *Mineralia Slovaca*, 54, 1, pp. 47–68.

BAJTOŠ, P. 2024: Increase in arsenic concentration in mine water at the flooded Slovinky copper mine – causes and consequences. *Groundwater*, 30, 1, pp. 38–61.

BAJTOŠ, P., MALÍK, P., ŠVASTA, J. 2013: Long-term impact of acid mine drainage on surface water chemistry at the Smolník Pyrite Mine. In: *Proceedings of the First International Conference on Mine Water Solutions in Extreme Environments, Lima, Peru*, pp. 285–298.

BAJTOŠ, P., MAŠLÁR, E., MAŠLÁROVÁ, I., SISKA, M. 2023: Partial Monitoring System – Geological Factors. Subsystem 04: Impact of Mineral Extraction on the Environment. Report for 2022. Available online: https://dionysos.geology.sk/cmsgf/

BAJTOŠ, P., MAŠLÁR, E., MAŠLÁROVÁ, I., SISKA, M. 2024: Partial Monitoring System – Geological Factors. Subsystem 04: Impact of Mineral Extraction on the Environment. Report for 2023. Available online: https://dionysos.geology.sk/cmsgf/

BAJTOŠ, P., MAŠLÁR, E., MAŠLÁROVÁ, I., SISKA, M. 2025: Partial Monitoring System – Geological Factors. Subsystem 04: Impact of Mineral Extraction on the Environment. Report for 2024. Available online: https://dionysos.geology.sk/cmsgf/

BALINTOVA, M., JUNAKOVA, N., CHERNISH, Y. 2023: The Influence of Acidic Mine Waters on Physico-Chemical Processes in the Aquatic Environment. *Engineering Proceeding*, 57, 1, https://doi.org/10.3390/engproc2023057004.

BHATTACHARYA, A.B., MUKHERJEE, J., BUNDSCHUH, R., ZEVENHOVEN, R.H., LOEPPERT (Eds.) 2007: Arsenic in Soil and Groundwater Environment. *Trace Metals and other Contaminants in the Environment*, 9, pp. 441–472.

DEMCHAK, J., SKOUSEN, J.G., MCDONALD, L.M. 2004: Longevity of Acid Discharges from Underground Mines Located above the Regional Water Table. *Journal of Environmental Quality*, 33, 2, pp. 656–668.

DEUTSCH, W.J. 1997: *Groundwater Geochemistry: Fundamentals and Applications to Contamination*. Boca Raton, CRC Press, 232 p.

DIXIT S, HERING J.G. 2003: Comparison of arsenic(V) and arsenic(III) sorption onto iron oxide minerals: implications for arsenic mobility. *Environmental Sciences & Technology*, 37, 18, pp. 4182–4189.

EHRLICH, H.L. 1996: *Geomicrobiology*. 3rd ed. New York, Marcel Dekker, 719 p.

FINTA, B., ROZDOBUĎKOVÁ, N. 1987: Reduction of the negative impact of the Smolník ironworks on water bodies. Final stage report on the RVT K 0199-65-05-03 economic plan. Manuscript – Institute for Ore Research, Mníšek pod Brdy, Košice branch.

GRECULA (Ed.), ABONYI, A., ABONYIOVÁ, M., ANTAŠ, J., BARTALSKÝ, B., BARTALSKÝ, J., DIANIŠKA, I., DRNDZÍK, E., ĎUĎA, R., GARGULÁK, M., GAZDAČKO, Ľ., HUDÁČEK, J., KOBULSKÝ, J., LÖRINCZ, L., MACKO, J., NÁVESŇÁK, D., NÉMETH, Z., NOVOTNÝ, L., RADVANEC, M., ROJKOVIČ, I., ROZLOŽNÍK, L., ROZLOŽNÍK, O., VARČEK, C., ZLOCHA, J. 1995: *Mineral deposits* of the Slovak Ore Mountains. Volume 1. Bratislava, Mineralia Slovaca – Monograph, 834 pp.

GRECULA, P., KOBULSKÝ, J., GAZDAČKO, Ľ., NÉMETH, Z., HRAŠKO, Ľ., NOVOTNÝ, L., MAGLAY, J., PRAMUKA, S., RADVANEC, M., KUCHARIČ, Ľ., BAJTOŠ, P., ZÁHOROVÁ, Ľ. 2011: *Explanatory notes to the geological map of the Spiš-Gemer Ore Mountains 1:50,000*. Bratislava, ŠGÚDŠ, 308 pp.

GRECULA, P., KOBULSKÝ, J., GAZDAČKO, Ľ., NÉMETH, Z., HRAŠKO, Ľ., NOVOTNÝ, J., MAGLAY, J. 2009: *Geological map of the Spiš-Gemer Ore Mountains at a scale of 1:50,000*. Bratislava, ŠGÚDŠ.

GRMELA, A. 1998: The issue of high iron concentrations in mine waters from decommissioned mines in the Lower Silesian Coal Basin. In: *Proceedings of the conference Transport of inorganic pollutants in groundwater*. Ostrava, VŠB-TU Ostrava. HANZEL, V. (Ed.) 1998: Geological Dictionary. Hydrogeology. Bratislava, Dionýz Štúr Publishing House, 301 pp.

HOMOLA, V., KLÍR, S. 1975: *Hydrogeology of the Czechoslovak Socialist Republic III. Hydrogeology of Mineral Deposits*. Prague, ACADEMIA, 426 pp.

JELEŇ, M., LÖRINCZ, L., BACHŇÁK, M., PALČO, A. 1993: Kobeliarovo – Transport Tunnel – Documentation. Final Report. Manuscript – Archive of the State Geological Survey of Slovakia, Bratislava.

JETEL, J. 1982: Determination of Rock Hydraulic Parameters by Hydrodynamic Tests in Boreholes. Knih. ÚÚG, 58, Prague, 248 pp. KIM, CH.S., HAN, U.CH., SIN, H., HWANG, S.R., WANG, J.M. 2024: Thermodynamic Behaviour of Pyrite and Arsenopyrite in Preoxidation for Chlorination Leaching of Refractory Gold Concentrate. *Hindawi Journal of Chemistry*, 2024, Article ID 2671023, 9 pp.

KUPKA, D., PÁLLOVÁ, Z., HORŇÁKOVÁ, A., ACHIMOVIČOVÁ, M., KAVEČANSKÝ, V. 2012: Effluent water quality and the ochre deposit characteristics of the abandoned Smolník mine, East Slovakia. *Acta Montanistica Slovaca*, 17, 1, pp. 56–64.

LI, X., JIN, Z., BAI, G., WANG, J., GAO, F., LINGHU, J. 2020: Experimental study on the influence of water immersion on spontaneous combustion of anthracite with high concentrations of sulphur-bearing minerals. *Journal of Thermal Analysis and Calorimetry*, 141, pp. 893–903.

LINTNEROVÁ, O., ŠOTTNÍK, P., ŠOLTÉS, S. 2008: The abandoned Smolnik mine (Slovakia) and a catchment area affected by mining activities. *Estonian Journal of Earth Sciences*, 57, 2, pp. 104–110.

LOTTERMOSER, B.G. 2010: *Mine Wastes*. 3rd ed. Berlin Heidelberg, Springer-Verlag, 404 p.

LÖRINCZ, L., ŠVANTNEROVÁ, E., ŠČUKA, J., MIHALÍK, F., STUPÁK, J., ÚJPÁL, J., JELEŇ, M., LEŠKA, S. 1989: Nižná Slaná – surroundings, metasomatic siderite. Manuscript – archive of Geofond ŠGÚDŠ Bratislava, 169 pp.

LEUZ A.K., MÖNCH H., JOHNSON C.A. 2006: Sorption of Sb(III) and Sb(V) onto goethite: influence on Sb(III) oxidation and mobilisation. *Environmental Sciences & Technology*, 40, 23, pp. 7277–7282.

LUKÁČ, S. 2002: Raw material base and the state of mining and processing technology at the Siderit Nižná Slaná plant. *Acta Montanistica Slovaca*, 7, 4, pp. 227–230.

MASSCHELEYN, P.H., PATRICK, W.H. Jr. 1994: Selenium, arsenic and chromium redox chemistry in wetland soils and sediments. *Environmental Geochemistry and Health*, 16, Special issue, pp. 615–625.

MIHÓK, J. 1994: Reclassification of the Nižná Slaná deposits. Manuscript – archive of Geofond ŠGÚDŠ Bratislava.

MIHÓK, J. 1997a: Geology of the Nižná Slaná deposit and its surroundings. In: *Proceedings of the 9th International Mining Conference*. Košice, pp. 61–67.

MIHÓK, J. 1997b: SIDERIT Nižná Slaná Mining and Processing Plant. *Acta Montanistica Slovaca*, 2, 2, pp. 125–136.

MIHÓK, J., JANČURA, M. 2000: Final report and calculation of reserves for the geological exploration project "Nižná Slaná – Mano – Gabriela deposit, XIIth horizon, PoP stage". Manuscript – archive of Geofond, ŠGÚDŠ Bratislava.

MIKLÓS, L., HRNČIAROVÁ, T. (Eds.) 2002: Atlas of the Slovak Republic. 1st ed. Bratislava, Ministry of the Environment of the Slovak Republic, Banská Bystrica, Slovak Environmental Agency, 344 pp.

MOK, W.M., WAI, C.M. 1994: *Mobilisation of arsenic in contaminated river waters*. In: *Nriagu, J.O. (Ed.):* Arsenic in the environment. Part I. Cycling and characterisation. New York, John Wiley Int., pp. 99–108.

MOSES, C.O., NORDSTROM, D.K., HERMAN, J.S., MILLS, A.L. 1987: Aqueous pyrite oxidation by dissolved oxygen and by ferric iron. *Geochimica et Cosmochimica Acta*, 51, 6, pp. 1561–1571.

NORDSTROM, D.K., ALPERS, C.N. 1999: *Geochemistry of acid mine waters*. In: Plumlee, G.S., Logsdon, M.J. (Eds): The Environmental Geochemistry of Mineral Deposits. Reviews in Economic Geology 6A, Society of Economic Geologists, pp. 133–160.

NORDSTROM, D.K., SOUTHAM, G. 1997: *Geomicrobiology of sulphide mineral oxidation*. In: Banfield, J.F., Nealson, K.H. (Eds.): Geomicrobiology: Interactions between Microbes and Minerals. Reviews in Mineralogy, 35, pp. 361–390.

ONIFADE, M., GENC, B. 2019: Spontaneous combustion liability of coal and coal-shale: a review of prediction methods. *International Journal of Coal Sciences & Technology*, 6, 2, pp. 151–168.

PARKHURST D.L., APPELO C.A.J. 2013: *Description of input and examples for PHREEQC version 3 – A computer program for speciation, batch-reaction, one-dimensional transport, and inverse geochemical calculations*. U.S. Geological Survey Techniques and Methods, book 6, chap. A43, 497 p.

PIERCE, M.L., MOORE, C.B. 1982: Adsorption of arsenite and arsenate on amorphous iron hydroxide. *Water Research*, 16, 7, pp. 1247–1253.

PITTER, P. 1999: *Hydrochemistry.* 3rd ed. Prague, University of Chemistry and Technology, 568 pp.

ROBERTSON, F.N. 1989: Arsenic in groundwater under oxidising conditions, south-western United States. Environmental Geochemistry and Health, 11, pp. 171–185.

ROSENBLUM, F., NESSET, J., SPIRA, P. 2001: Evaluation and control of self-heating in sulphide concentrates. *CIM Bulletin*, 94, pp. 92–99.

SCHERER S., MALÍK, P., BAJTOŠ, P., GEDEON, M., KORDÍK, J. 1999: Hydrogeological and hydrogeochemical map of the northern part of the Spiš-Gemer Ore Mountains at a scale of 1:50,000. Manuscript – archive of Geofond ŠGÚDŠ Bratislava.

SINGER, P.C., STUMM, W. 1970: Acid Mine Drainage – Rate-Determining Step. *Science*, 167, pp. 1121–1123.

SMEDLEY, P.L., ZHANG, M., ZHANG, G., LOU, Z. 2003: Mobilisation of arsenic and other trace elements in fluviolactustrine aquifers in the Huhhot Basin, Inner Mongolia. *Applied Geochemistry*, 18, 9, pp. 1453–1477.

Directive of the Ministry of the Environment of the Slovak Republic of 28 January 2015 No. 1/2015 – 7 on the preparation of a risk analysis of contaminated sites.

STRÍČEK, I., JANKULÁR, M., KORDÍK, J., KONEČNÝ, P. 2022: The impact of mine drainage on the sediments of the Slaná River. In: *Jurkovič, Ľ., Kordík, J., Čičáková, C. (Eds.): Proceedings of the Geochemistry 2022 Conference, Piešťany 30 November–2 December 2022*. Bratislava, ŠGÚDŠ, pp. 98–101.

STRÍČEK, I., JANKULÁR, M., KORDÍK, J., GYÖRÖG, I. 2024: Monitoring the impact of mine drainage on the sediments of the Slaná River. *Jurkovič, Ľ., Kordík, J., Čičáková, C. (Eds.): Proceedings of the Geochemistry 2024 Conference, Bratislava, 10–11 April 2024*. Bratislava, ŠGÚDŠ, pp. 160–161.

SUCHÁR, A., ZBORŇÁK, V. 1962: Nižná Slaná – Fe, ZS and VZ. Manuscript – archive of Geofond ŠGÚDŠ Bratislava.

SUCHÁR, A., ZBORŇÁK, V. 1966: Nižná Slaná – Fe (Manó-Gabriela), ZS and VZ. Manuscript – Geofond archive, ŠGÚDŠ Bratislava.

TOMETZ, L., KYSEĽOVÁ, K. 2009: Quantity and quality of groundwater at the Mária mine and their relationship to the revitalisation of mineral extraction. *Groundwater*, 15, 2, pp. 162–173.

TURAN, J., TURANOVÁ, L. 1993: Carbonate mineralisation of the Nižná Slaná deposit. *Western Carpathians. Series: Mineralogy, Petrography, Geochemistry, Metallogeny*, 16, pp. 147–167.

TURANOVÁ, L., KHUN, M., TURAN, J. 1995a: Geochemistry of black shales in selected areas. *Geological Works*, *Reports*, 100, pp. 105–115.

TURANOVÁ, L., KHUN, M., TURAN, J., ČELKOVÁ, A. 1995b: Heavy metals in black shales of the deposit areas of the Western Carpathians and their impact on the environment. *Mineralia Slovaca*, 27, 2, pp. 99–105.

TURANOVÁ, L., TURAN, J., DEPTA, M. 1992: The Accessories in the "Black Shales" of the Siderite Deposits from the Spišsko-gemerské rudohorie Mts. In: *Kfek, B. (Ed.): Metallogeny and anoxic Environments*, Prague, pp. 51–54.

WIESE, R.G., POWELL, M.A., FYFE, W.S. 1987: Spontaneous formation of hydrated iron sulphates on laboratory samples of pyrite- and marcasite-bearing coals. *Chemical Geology*, 63, 1-2, pp. 29–38.

WELCH, A.H., LICO, M.S. 1998: Factors controlling As and U in shallow groundwater, southern Carson Desert, Nevada. *Applied Geochemistry*, 13, 4, pp. 521–539.

WOLKERSDORFER, CH. 2008: *Water Management at Abandoned Flooded Underground Mines. Fundamentals, Tracer Tests, Modelling, Water Treatment*. Berlin Heidelberg, Springer-Verlag, 465 p.

YOUNGER, P.L. 1997: The longevity of minewater pollution – a basis for decision-making. *Science of the Total Environment*, 194-195, pp. 457-466.

SUMMARY

The chemical composition and discharge rate of mine water flowing from the Manó-Gabriela siderite mine (Slovak Ore Mountains, eastern Slovakia) were monitored from the complete flooding of the mine in February 2022 until the end of 2024. The initially low-mineralised, slightly alkaline water that began to overflow from the shaft after the mine was flooded acquired, within less than ten days, the character of highly mineralised (40 $^{g \cdot L^{-1}}$), acidic mine water with extremely high concentrations of sulphates, Mg, Fe, Mn, As, Ni, as well as elevated levels of Co, Al and Zn (Tables 4 and 5; Figs. 3–8). This change reflected the vertical stratification of water that developed in the Gabriela shaft during the flooding as a result of the inflow of low-mineralised, shallow-circulating groundwater from the Jozef adit.

During the subsequent period, two major changes in flow conditions occurred in the mine, each reflected in changes in the temperature and chemical composition of water discharging from the Gabriela shaft. The first change was related to a technical intervention undertaken in June 2022 to stop the inflow – approximately 16 $^{L \cdot s^{-1}}$ – of water flowing from

the Kobeliarovský corridor and entering the central part of the Manó-Gabriela mine via the blind raise by the Manó II shaft. The second change was probably the result of renewed inflow, due to seepage through a dam, of a portion of the stream flowing through the Kobeliarovský corridor – estimated at about 2 $L \cdot s^{-1}$ – into the blind raise by the Manó II shaft. In both cases, the most significant change was in water temperature (a decrease from 36 °C to 17 °C and an increase from 18 °C to 34 °C, respectively). Pronounced changes also occurred in the concentrations of sulphates (a decrease from 40 $g \cdot L^{-1}$ to 26 $g \cdot L^{-1}$ and an increase from 24 $g \cdot L^{-1}$ to 30 $g \cdot L^{-1}$) and Mg (a decrease from 6 $g \cdot L^{-1}$ to 5 $g \cdot L^{-1}$ and an increase from 5 $g \cdot L^{-1}$ to 6 $g \cdot L^{-1}$) (Figs. 3 and 4). These changes in mine-water flow, however, had no significant effect on Fe and Mn concentrations, which exhibited a steady decrease with a statistically significant exponential trend throughout the entire monitoring period (Fig. 5). A statistically significant downward trend – consistent with the expected first-flush behaviour – was also documented for total mineralisation, sulphates, Mg, Al and Zn during the part of the monitoring period following the second flow regime change. During this interval, Co concentrations and pH showed statistically significant upward trends. Arsenic concentrations were highly variable over time, likely reflecting pronounced spatial variability in the source minerals within the mine (Fig. 7).

The quantities of Fe, Mn, As and Ni present in this water cause severe contamination of the surface water of the Slaná River, which receives the mine discharge, even though the Gabriela shaft water mixes with clean water from the Kobeliarovský crosscut prior to reaching the surface. Evaluation of the magnitude of this impact is beyond the scope of this paper.

Geochemical calculations using PHREEQC (Tables 7–9; Fig. 10), interpreted in the context of current knowledge of the studied system and site conditions, indicate that the dominant hydrogeochemical processes controlling the chemical composition of the mine water are the dissolution of Fe carbonates in the ore body combined with the oxidation of sulphides, particularly pyrite and arsenopyrite (Eqs. 1–9). The intensity of carbonate dissolution is strongly influenced by protons generated during sulphide oxidation and by the relatively high partial pressure of $_{CO_2}$ (0.29–0.98 atm, as indicated by saturation indices in the samples – Table 8; Fig. 10). The nature of these processes differs markedly between the unsaturated and water-saturated (flooded) parts of the mine. In the environment of waste piles composed of black phyllites left inside the workings, acidic solutions (AMD/ARD) may have formed, intensifying the dissolution of ore carbonates beyond the levels typical for a siderite mine of an analogous genetic type. In addition, spontaneous heating leading to the combustion of pyrite occurred here, enhanced by the presence of organic carbon in the phyllites. These thermal processes could, beyond ordinary atmospheric conditions in the mine: (1) create, at temperatures up to 80 °C, local temperature optima for microorganisms that accelerate pyrite oxidation; (2) increase acidity (condensates of thermally released SO_2 and CO_2 further intensified carbonate dissolution); and (3) increase the amount of secondary sulphates, thereby raising water mineralisation after mine flooding. The combustion of black phyllites likely also released arsenic vapours, the condensation of which contributed to elevated arsenic concentrations in the mine water. The extent to which these processes contribute to the high mineralisation of the water, however, cannot be quantified more precisely with the available data.

Speciation calculations for arsenic in the mine water of Manó-Gabriela show that it occurs almost exclusively in oxidation state +5, with $H_2AsO_4^-$ dominating over $HAsO_4^{2-}$, whilst the neutral complex H_3AsO_4 is negligible and the anion AsO_4^{3-} is absent (Table 10). Nickel in the Gabriela shaft water occurs predominantly as the neutral complex $NiSO_4$ (49–69%), followed by Ni^{2+} (22–44%), and the complexes $NiHCO_3^+$ (3–6%) and $Ni(SO_4)_2^{2-}$ (0.3–4.5%)
(Table 11).

For the prognosis of the future development of the chemical composition of the mine water flowing through the Gabriela shaft, it is important to consider the possible influence of the thermolift on the flow of water in the flooded (saturated) part of the mine. The zones of overheated rock mass created as a result of the burning of the collapses could generate an upward current in the central part of the mine and influence deep circulation, which prevents the development of water stratification with a stable upper layer of less mineralised water, which would be favourable from an environmental perspective. The duration of this impact and its persistence to the present day remain unspecified. However, it is also possible that the ongoing influence of the processes of spontaneous heating of pyrite, occurring in mining areas just above the water surface, on the circulation and chemical composition of the water in the Manó–Gabriela mine, continues to this day.

To gain a better understanding of the hydrogeochemical processes occurring in the mine, it is necessary to monitor and continuously assess vertical changes in the chemical composition, redox conditions and temperature of the mine water at accessible locations. To better explain the high temperature of the water flowing out of the Gabriela shaft, it is necessary to study the geothermal conditions of the mine using model calculations of heat accumulation in rocks and their exchange with mine water following the flooding of hot heaps, supported by vertical profiles of the water temperature in the mine and measurements of the $_{CO_2}$ and $_{SO_2}$ content in the mine air. In principle, however, it is possible to assume a gradual, slow decrease in its temperature, mineralisation and the content of environmentally hazardous elements dissolved in it over the coming period.